Title

Cranial base and facial morphology and severity of clefting: a geometric morphometric analysis

ISBN
9798247945819

Author
Ran-Sukkawala, Marrina Ruomei

Publication Date
2026-06-03

Peer reviewed|Thesis/dissertation

Cranial base and facial morphology and severity of clefting: a geometric morphometric analysis

by
Marrina Ran-Sukkawala

THESIS
Submitted in partial satisfaction of the requirements for degree of
MASTER OF SCIENCE

in

Oral and Craniofacial Sciences

in the

GRADUATE DIVISION
of the
UNIVERSITY OF CALIFORNIA, SAN FRANCISCO

Approved:

DocuSigned by:
Snehlata Oberoi
5341FCF07489402...

Snehlata Oberoi
Chair

DocuSigned by:
Nathan Young
8A9E0B3A22D404...

Nathan Young

Signed by:
Yeumin Hong
CE6EAA6FBA31451...

Yeumin Hong

Committee Members

Cranial base and facial morphology and severity of clefting: a geometric morphometrics analysis

Marrina Ran-Sukkawala

Abstract

Background: Cleft lip with or without cleft palate (CL/P) results from failed fusion of the facial prominences during embryogenesis. The cranial base, shaped largely by intrinsic developmental controls, serves as a practical proxy for the embryonic brain morphology that governs facial prominence positioning and fusion timing. Its relationship to CL/P severity in humans remains incompletely characterized.

Objectives: To compare basicranial and facial shape between CL/P and non-cleft individuals, quantify their morphological covariation, and determine whether these parameters correlate with cleft severity.

Materials and Methods: CBCT images from 30 children with nonsyndromic CL/P (ages 7–11), acquired prior to alveolar bone grafting or orthodontic treatment, were compared to 29 age- and sex-matched controls. Thirty-nine basicranial and 29 facial three-dimensional landmarks were placed and analyzed using geometric morphometrics in MorphoJ, including Procrustes superimposition, PCA, CVA, PLS analysis, and multivariate regression against cranial base width and flexure.

Results: CL/P individuals had basicrania that were wider anteriorly and in the middle, narrower posteriorly, and shorter in the anterior-to-posterior dimension. Their midfaces were wider and less anteriorly projecting. Anterior and middle cranial base width increased in the cleft group; posterior width was greater in controls. Cranial base flexure explained less variance than the width measures. PLS analysis confirmed significant basicranial-facial covariation: narrower, longer basicrania predicted longer, more projecting faces in controls, while wider, shorter basicrania predicted retruded midfaces in CL/P individuals. Asymmetry trends favored the CL/P group but did not reach significance, and no clear severity-specific relationship was established, likely due to limited subgroup sample sizes.

Conclusions: CL/P is associated with a distinct, quantifiable basicranial and facial morphological profile consistent with a wider anterior brain influencing facial prominence fusion. Significant basicranial-facial covariation supports their developmental integration. Early basicranial morphometrics may inform anticipation of midfacial retrusion, interceptive orthodontic timing, and surgical planning in CL/P patients.

Table of Contents

List of Figures

List of Tables

List of Abbreviations

ABG - alveolar bone grafting

ACBW – anterior cranial base width

CBCT - cone beam computed tomography

CL/P - cleft lip with or without cleft palate

CVA - Canonical Variate Analysis

GM - geometric morphometrics

MCBW – middle cranial base width

PCA - Principal Component Analysis

PCBW – posterior cranial base width

PLS - Partial Least Squares analysis

UCSF - University of California San Francisco

Introduction

Background

Craniofacial malformations occasionally arise during embryonic development as a consequence of disrupted morphogenetic processes. The human face emerges from five facial prominences surrounding the embryonic stomodeum: the frontonasal prominence (which subdivides into medial and lateral nasal processes), paired maxillary prominences, and paired mandibular prominences. Fusion between the medial nasal processes and maxillary prominences gives rise to the upper lip, primary palate, and secondary palate. Prior to this fusion, distinct grooves demarcate the five prominences, and failure of proper apposition at these sites results in a spectrum of structural malformations, including cleft lip and palate (Bush 2012).

Cleft lip (CL) arises between approximately 5 and 10 weeks in utero, resulting from failed fusion between the medial nasal and maxillary prominences. This failure may produce unilateral incomplete, unilateral complete, bilateral incomplete, or bilateral complete cleft lip. Separately, any disruption to the sequence of palatal shelf growth, elevation, or midline fusion during palatogenesis can result in cleft palate (CP) in its various forms (Bush 2012). Because these malformations originate during embryogenesis—a period inaccessible to direct clinical observation—researchers have increasingly turned to the cranial base as a proxy for understanding the developmental context in which orofacial clefts occur.

The co-development of the brain and face has been a foundational question in vertebrate evolutionary biology. As our understanding of craniofacial integration has grown, it has become clear that the morphogenesis of the brain and face are not independent processes but are instead intrinsically linked through shared tissue origins, physical adjacency, and molecular crosstalk (Marcucio et al. 2015). This perspective has motivated renewed interest in studying the cranial base—the bony interface between the brain and the face—as a window into the etiology of orofacial clefting.

Preliminary Studies

The developmental relationship between the brain and face operates through at least three distinct mechanisms: the common origin of their constituent tissues, the physical interactions that arise from their spatial adjacency, and the molecular signaling that governs their coordinated growth (Marcucio et al. 2015). Neural crest cells, which originate along the dorsal margin of the neural tube, populate the facial prominences and form the mesenchymal scaffold of the craniofacial skeleton. Concurrently, the brain itself serves as a structural platform that shapes the positioning of the facial primordia, and changes in brain size directly influence the timing and feasibility of prominence fusion (Marcucio et al. 2015). Understanding when and how clefting occurs therefore requires an appreciation of how facial changes relate to underlying brain morphology. Because brain shape cannot be measured directly at the embryonic stages when clefting occurs, the basicranium serves as a practical and theoretically justified proxy. The basicranium is a developmentally distinct module of the skull that undergoes endochondral ossification within its synchondroses, making its shape and growth more likely to be governed by intrinsic developmental controls rather than external functional pressures (Parsons et al. 2015). It ossifies early in craniofacial development, reaches adult size before the calvarium and face, and thereby sets the geometric parameters within which the rest of the skull grows. Centrally located and forming the floor upon which the brain rests, the basicranium is widely considered to be central to growth and patterning of the skull as a whole (Parsons et al. 2015).

Structurally, the basicranium is composed of two functional units: the midline basicranium, which is predominantly influenced by brain size, and the lateral basicranium, which is more strongly associated with facial shape (Neaux et al. 2019). Using three-dimensional landmarks placed on CT scans of primate crania, Neaux et al. (2019) demonstrated significant morphological integration not only between the lateral basicranium and the face, but also between the midline basicranium and the face—findings that support a pervasive, rather than compartmentalized, relationship across these craniofacial structures. In individuals with cleft lip and/or palate (CL/P), this integration appears to manifest asymmetrically: the lateral cranial base is more morphologically affected than the middle basicranium, while transverse facial and basicranial dimensions are comparatively less dysplastic (Jahanbin et al. 2015). These findings underscore the basicranium as a structure that exhibits shape changes in concert with associated facial malformations.

Additional evidence for basicranial-facial covariation comes from a study by Romash et al. (2017), which used three-dimensional landmarks to characterize the basicranium and facial skeleton in cleft patients at the University of California, San Francisco (UCSF) and in a corresponding mouse model. Asymmetric variation between the basicranium and face was found to covary significantly in both species, suggesting that basicranial shape influences facial asymmetry in an additive fashion: the side of the skull with a larger basicranium corresponds to a larger hemiface (Romash et al. 2017). This work has contributed to our growing interest in the integrated study of craniofacial features, and the present study builds directly upon this framework.

The brain is among the earliest structures to develop in the embryo, and its early growth makes it a guiding influence on the spatial positioning and morphology of the facial primordia throughout development. Work by Parsons et al. (2011) demonstrated that phenotypic variation in the forebrain is highly correlated with facial shape during face formation in mice. Specifically, variation in forebrain size was correlated with the degree of prognathism and with the orientation of the facial prominences, suggesting that the integration of the brain and face is directly relevant to the etiology of midfacial malformations such as orofacial clefts (Parsons et al. 2011). Complementing this, Boughner et al. (2008) studied mice carrying Crf4 mutations that produce variation in facial length, and found that this short-faced phenotype was accompanied by a significant reduction in both brain size and basicranial length—effects that were already detectable at embryonic stages of face formation. Mechanistically, a narrower or smaller forebrain reduces the physical gap that the facial prominences must traverse to achieve fusion, thereby altering the timing and morphology of primary palate formation (Boughner et al. 2008; Parsons et al. 2011).

These structural interactions are complemented by molecular signaling between the developing brain and face. Sonic hedgehog (SHH) signaling from the forebrain establishes the Frontonasal Ectodermal Zone (FEZ), a signaling center in the overlying facial ectoderm that maintains outgrowth of the central midface during face formation (Marcucio et al. 2015). Disruption of this molecular axis has downstream consequences for facial morphogenesis and is associated with a range of craniofacial malformations. These findings collectively reinforce the view that the face does not develop independently of the brain—rather, its form is substantially shaped by what lies beneath it.

Evidence for a brain phenotype in individuals with orofacial clefting extends beyond animal models into human populations. Weinberg et al. (2009) used three-dimensional morphometric analysis of magnetic resonance imaging (MRI) scans to compare brain shape in individuals with nonsyndromic orofacial clefting (NSOFC) against unaffected controls. Significant differences in brain shape were identified across all cleft groups, and when comparing individuals with cleft lip with or without cleft palate to non-cleft individuals, the brain shape differences were consistent and reproducible. These findings support the interpretation that the neuroanatomical phenotype observed in NSOFC individuals reflects a primary developmental manifestation of the defect—not a secondarily acquired characteristic—and is therefore likely rooted in the same embryonic processes that give rise to facial clefting (Weinberg et al. 2009).

Cranial base morphology in non-syndromic cleft lip and palate has also been characterized in clinical populations. Documented abnormalities include an increased cranial base angle, greater cranial base width, increased distance between the greater wings of the sphenoid, a smaller sella turcica, and a higher incidence of morphological variants of the sella turcica compared to unaffected controls (Utsunomiya et al. 2025). These structural differences, detectable radiographically, further establish the cranial base as a site of measurable morphological divergence in cleft populations and strengthen the rationale for using basicranial morphology as a proxy for understanding the developmental environment in which orofacial clefts arise.

Present Study

The aim of this retrospective study is to determine whether a correlation exists between the presence and severity of clefting and the shape of the cranial base and face, using geometric morphometrics (GM) as the primary analytical tool. Because cleft lip and palate originates during embryogenesis and the relevant developmental events cannot be observed directly in vivo, we approximate brain shape at the earliest clinically available time point using cone-beam computed tomography (CBCT) images of the basicranium. CBCT scans from patients with cleft lip with or without cleft palate (CL/P) seen at the UCSF Division of Orthodontics—all acquired prior to alveolar bone grafting (ABG)—are used for this purpose. Basicranial and facial landmarks will be placed using Amira, Landmark, and MorphoJ software, and shape variation will be analyzed via GM.

GM is a statistical framework specifically designed for the analysis of shape, defined as all geometric information remaining after the effects of position, size, and orientation are removed (Rutland et al. 2021). Its ability to capture shape variation while controlling for differences in structure size and imaging conditions makes it particularly well-suited to the study of complex craniofacial phenotypes.

By approximately age 5, the cranial base has completed roughly 90% of its growth, with the remaining 10% occurring over the subsequent decade (Moore 1974). We therefore use CBCT scans acquired at approximately 7–8 years of age—immediately prior to ABG, which is typically performed between ages 8 and 10—as our earliest available window into basicranial morphology. At this age, CL/P patients have typically undergone only soft tissue repair, with no alveolar bone grafting or orthodontic treatment yet performed. This minimizes the opportunity for post-developmental interventions to confound basicranial morphology and brings us as close as practicably possible to the developmental period of interest. The midline basicranium, notably, reaches adult-like maturity at approximately 7–8 years of age (Neaux et al. 2019), further supporting the interpretive value of this time point.

Aims

In this retrospective study, we aim to characterize the width, flexure, asymmetry, and overall shape of the cranial base across cleft severity groups and compare them to a non-cleft group. We also aim to assess the overall shape and asymmetry of the face, and to examine the degree of covariation between basicranial and facial morphology in individuals with and without CL/P.

Hypotheses

Null hypothesis: There is no correlation between severity of clefting and cranial base or facial shape.

Alternate hypotheses: (1) There is a significant correlation between presence and severity of clefting and cranial base shape. (2) As cleft severity increases, cranial base width increases. (3) There is a correlation between presence and severity of clefting and flexure of the cranial base. (4) As cleft severity increases, basicranial asymmetry increases. (5) Basicranial shape and facial shape covary significantly when comparing individuals with clefting versus those without clefting. (6) There is a correlation between presence and severity of clefting and facial shape. (7) As cleft severity increases, facial asymmetry increases.

Identifying asymmetries, differences in flexure, and relative width of the basicranium early in the growth period may provide clinically meaningful predictors of risk for developing lateral facial asymmetries and skeletal malocclusion. A deeper understanding of the relationship between cleft severity and cranial base and facial morphology has the potential to inform earlier and more targeted clinical intervention strategies.

Materials and Methods

A data set of individuals with diagnosis of clefting, including but not limited to: unilateral cleft lip with or without cleft palate (UCL/P), bilateral cleft lip with or without cleft palate (BCL/P), isolated cleft palate (CP), isolated cleft lip (CL) was obtained from the University of California San Francisco (UCSF)'s electronic health records (Apex/Epic). Cone beam computed tomography (CBCT) images from 30 individuals with cleft lip with or without cleft palate (CL/P) aged 7-11 years were compared to 29 age- and sex-matched controls without clefts.

The electronic health records of the individuals were reviewed, and the CL/P individuals' cleft types were ranked by numbers in order of severity of clefting. See Table 1 for severity of cleft type ranked by number, ranging from 1 (least severe, microform cleft lip), to 15 (most severe, bilateral complete cleft lip and palate).

Charts were reviewed to ensure that these CBCT images were taken prior to initiation of any orthodontic treatment or alveolar bone grafting (ABG). Our inclusion criteria were: nonsyndromic CL/P, no prior history of ABG or orthodontic treatment, and soft tissue repair was done at UCSF, to standardize the type of repair. Our exclusion criteria were: syndromic CL/P, prior history of alveolar bone grafting or orthodontic treatment, and soft tissue repair done outside UCSF.

39 landmarks on the cleft and control basicrania were placed to study correlation between severity of clefting and shape, width, flexure, and asymmetry of the basicrania. Landmarks were placed in the midline, anterior and posterior bilaterally. See Table 2 for

a complete list of basicrania landmarks. See Figure 1 for an example of a landmarked basicranium. 29 landmarks on the cleft and control faces were placed to study facial shape and asymmetry as measures of severity of clefting. See Table 3 for a complete list of facial landmarks. See Figure 2 for an example of a landmarked face.

The CBCT images were taken as part of routine pre-orthodontic records at the University of California, San Francisco Division of Orthodontics. The images were then exported as DICOM files and imported into Amira software. A threshold was identified for each CBCT that allowed the basicrania and face to be visualized as much as possible. Once the threshold was identified, a .surf file was generated for each image.

Each .surf file was converted to a .ply file by 3D Object Converter and landmarked using Landmark software. The same three people placed all the landmarks, and then the landmarks were all checked by the same person for consistency. The data quality of the landmarks was checked in MorphoJ, and MorphoJ was then used to perform geometric morphometrics (GM) analysis, including Procrustes superimposition and Principal Component Analysis (PCA) to assess shape. Statistical analysis was performed using partial least squares analysis (PLS) and multivariate linear regression analysis to test for correlation between presence and severity of clefting and morphology of basicrania and faces. Specifically, for the basicranium, we examined the following covariates (continuous quantitative variables): anterior cranial base width (distance between landmarks #5 and #6), middle cranial base width (distance between landmarks #3 and #4), posterior cranial base width (distance between landmarks #13 and #14), and flexure (SN-Basion angle, or angle between landmarks #16, #36, #38). For the face, we studied shape itself and asymmetry. The classifier variables (qualitative, categorical variables) we looked at were presence/absence of cleft and severity of cleft.

Results

Statistical Analysis

Principal Component Analysis

Shape variation across the sample was explored using Principal Component Analysis (PCA), a data reduction technique that transforms a large set of correlated shape variables into a smaller number of statistically independent axes of variation, termed principal components (PCs). Each PC is a linear combination of the original Procrustes shape coordinates, and they are ordered such that PC1 accounts for the greatest proportion of total shape variance in the sample, PC2 accounts for the second greatest, and so on. Because the PCs are orthogonal by construction, each captures a unique and non-overlapping dimension of shape variation. In the context of geometric morphometrics, plotting specimens along the first two or three PCs generates a morphospace in which the proximity of any two specimens reflects their degree of shape similarity. This visualization allows for identification of gross shape differences between cleft groups, detection of outliers, and assessment of overall sample structure, without presupposing any particular grouping or outcome. PCA is thus an exploratory tool: it describes the pattern of shape variation present in the data but does not test hypotheses about the relationship between shape and external variables such as cleft presence or severity.

Canonical Variates Analysis

Canonical Variates Analysis (CVA) was used to compare cranial base and facial shape between cleft and non-cleft individuals. While PCA identifies the axes of greatest overall shape variation within a sample regardless of group membership, CVA is specifically designed to find the axis of shape variation that best separates predefined groups from one another (Weinberg et al. 2009). In a two-group comparison such as cleft versus non-cleft, each specimen is assigned a score reflecting where it falls along this discriminating axis, and the degree of separation between the two groups' score distributions reflects the magnitude of shape difference between them.

An important advantage of CVA within a geometric morphometric framework is that shape variation along the canonical variate can be visualized directly as landmark displacements in three-dimensional space (Weinberg et al. 2009). This allows the specific regions of the cranial base and face that differ most between cleft and non-cleft individuals to be identified and interpreted in anatomical terms. Statistical significance of between-group shape differences was assessed using permutation testing, with significance set at $p < 0.05$. All CVA was performed in MorphoJ.

Partial Least Squares Analysis

To assess the degree of morphological integration between the cranial base and the face, two-block Partial Least Squares (PLS) analysis was utilized. Unlike PCA, which operates on a single block of variables, PLS is designed for the simultaneous analysis of two separate blocks of shape data — in this case, the basicranial landmark coordinates (Block 1) and the facial landmark coordinates (Block 2). The analysis identifies pairs of linear combinations, one from each block, that exhibit maximal covariation with one another. The first pair of singular axes (PLS1) accounts for the greatest covariance between the two blocks, with subsequent pairs accounting for progressively smaller proportions of the shared variance. The strength of the overall association between the two blocks is quantified by the RV coefficient, a multivariate analog of the Pearson correlation coefficient, which ranges from 0 (no integration) to 1 (perfect covariation). Statistical significance is assessed by permutation testing, in which the observed covariance is compared against a null distribution generated by randomly reassigning specimens across the two blocks. Scores along PLS1 for each block are plotted against one another to visualize the relationship: a tight, linear distribution of specimens in this plot indicates strong integration, meaning that a given basicranial shape reliably predicts a corresponding facial shape. This analysis directly tests the hypothesis that basicranial and facial shape covary in a structured way across individuals with differing cleft presence or severity.

Findings

Cleft vs. non-cleft basicrania

When looking at the basicranium data, we can see the cleft and non-cleft individuals have differences along PC1 and PC2, and most of the differences between the cleft and non-cleft basicrania is along PC2 (see Figure 3). The PC1 shape changes shows that the cleft individuals have narrower posterior cranial bases than non-cleft individuals (see Figure 4). The PC2 shape changes shows that the cleft basicrania are shorter and wider in the anterior, which is consistent with our hypothesis, indicating that cleft individuals may have a wider anterior brain early on in development (see Figure 5).

A Canonical Variate Analysis (CVA) was also performed for the cleft versus non-cleft basicrania. See Figure 6 for a bar graph displaying the Canonical Variate (CV) scores. See Figure 7 for the CV shape changes, which shows a combination of the findings we saw in PC1 and PC2: the basicrania of cleft individuals are narrower in the posterior cranial base, wider in the anterior cranial base, and are shorter in length.

CVA (Cleft vs. None, n = 59) statistics:

- Goodall's F = 6.9397, p < 0.0001 (10,000 permutations)
- Mahalanobis distance = 5.3898
- Procrustes distance = 0.0641

Cleft vs. non-cleft faces

When reviewing the facial data, we can see the cleft and non-cleft individuals have differences along PC1 and PC2, and most of the differences between the cleft and non-cleft faces is along PC1 (see Figure 8). The PC shape changes shows that the faces of cleft individuals are overall smaller, and the ears are wider than in non-cleft individuals. The cleft individuals have smaller and wider midfaces, which is consistent with the cleft basicrania being wider in the anterior cranial base area. The landmarks in the figure that appear to be going down are actually going in, which depicts the midface being smaller (see Figure 9).

Cleft vs. non-cleft basicrania and faces (Partial Least Squares Analysis)

A Partial Least Squares (PLS) analysis was also run, that shows the two parts within a configuration: the landmarks associated with the face (in blue) and the landmarks associated with the basicranium (in red). See Figure 10. This allows us to see where the variation in one block covaries with the variation in another block. Figure 11 shows that there is one axis that discriminates where most of the covariation between the face block and basicranium block occurs. Figure 12 shows the scores along PLS1 for each block plotted against one another to visualize the relationship, and the non-cleft individuals being visually separated from the cleft individuals.

The PLS1 shape changes shows that positive scores along PLS1 are more associated with non-cleft individuals, and these individuals tend to have narrower, longer, and overall more projecting, larger faces. In these individuals, we can see that as the basicranium becomes narrower, the face becomes longer (see Figure 13).

We see the opposite finding in cleft individuals; these individuals tend to have wider anterior and middle cranial bases and shorter (in the anterior to posterior direction) basicrania. They also tend to have more retruded external faces, or in other words, smaller, less projecting midfaces (see Figure 14).

If we assume the landmarks on the ears and cheeks are less associated with the brain and basicranium than are the landmarks on the midface and mouth area, and we run the Partial Least Squares analysis with only the landmarks on the midface and mouth area in order to focus on the landmarks relative to the basicranium, we get similar results; see Figure 15. As the basicranium gets narrower, the face gets longer, and these individuals tend to be non-cleft. As the anterior cranial fossa becomes wider and the basicranium becomes shorter in length, the midface also tends to become shorter and less projecting, and these individuals tend to have clefts. See Figure 16. This relationship holding whether or not peripheral facial landmarks (ears, cheeks) were included indicates that the core association is driven by midface and mouth-region morphology rather than artifact of landmark selection.

Two-Block PLS (Basicranium vs. Face, n = 59) statistics:

- RV coefficient = 0.567, $p < 0.001$ (250 permutations)
- PLS1: 65.9% of total covariance, $r = 0.927$, $p < 0.001$
- PLS2: 15.4% of covariance, $r = 0.780$, $p = 0.008$

Cranial base width and flexure (regression analysis)

We regressed the basicranium data with anterior cranial base width (ACBW), middle cranial base width (MCBW), posterior cranial base width (PCBW), and flexure of cranial base (SN-Basion angle).

When we regress the basicranium with ACBW, we see that in general as ACBW increases or gets wider, there is more clefting (see Figure 17). The shape changes in Figure 18 show that as the basicranium gets wider, it also gets a little shorter in the occipital region, and not much in the midline area.

When we regress the basicranium with MCBW, we see that in general as MCBW increases, there is more clefting, though not as strong of a relationship as with ACBW. See Figure 19. The shape changes in Figure 20 show that as the basicranium gets wider, it also gets a little shorter in the occipital region, and not much in the midline area, similar to the findings in the ACBW regression.

When we regress the basicranium with PCBW, we see that as PCBW decreases or gets narrower, there is more clefting (see Figure 21). The non-cleft individuals tend to have wider PCBW, and the cleft individuals tend to have narrower PCBW. See Figure 22 for the shape changes.

When we regress the basicranium with flexure of cranial base (SN-Basion angle), we see that flexure explains notably less variance than the cranial base width measures (see Figure 23), though all regressions are significant at $p < 0.05$. See Figure 24 for the shape changes.

Regressions — Full Sample (n = 59):

Predictor	% Variance Explained	p-value
ACBW	10.00%	< 0.0001
MCBW	8.77%	< 0.0001
PCBW	14.52%	< 0.0001
Flexure	4.27%	0.0037

Cleft severity

The CL/P individuals' cleft types were ranked by numbers in order of severity of clefting. See Table 1 for severity of cleft type ranked by number, ranging from 1 (least severe, microform cleft lip), to 15 (most severe, bilateral complete cleft lip and palate). When we regress the cleft basicrania with ACBW, MCBW, PCBW, and flexure of cranial base, we do not see a clear relationship between cleft severity and these covariates (See Figures 25, 26, 27, 28). Figure 29 shows the PLS scores for the basicranium block and face block, colored by cleft severity. From this, we also cannot conclude that there is a relationship between cranial base or facial morphology and cleft severity, though a larger sample size with more individuals per cleft type may be more conclusive.

Regressions — Cleft Only (n = 30):

Predictor	% Variance Explained	p-value
ACBW	8.10%	0.0062
MCBW	12.65%	< 0.0001
PCBW	19.18%	< 0.0001
Flexure	7.11%	0.0141

Asymmetry

We also ran a Principal Component Analysis to look at the asymmetry of the face and basicrania data set to see if there is a difference between the cleft and non-cleft groups. Figure 30 shows that the cleft group may be a little more asymmetric than the non-cleft group. We also separated it into side of cleft (none, midline, unilateral, or bilateral) which can be seen in Figure 31. Most clefts occur on the left side, and there was only one individual in our study with the cleft occurring on the right side, which is why we used the unilateral or bilateral category instead of distinguishing right side from left side. Figure 32 shows the PC scores of the asymmetric shape component separated further by cleft severity. Overall, we cannot conclude that there is a significant relationship between cleft severity and asymmetry. A larger sample size with more individuals per cleft type may be more conclusive.

Discussion

Regarding sample size - for two of the cleft subjects that had their basicrania landmarked, we had to omit their faces from the data because the chin and forehead restraints from the CBCT machine were blocking too many of the facial landmarks. For some of the faces that we did include, some landmarks were missing and then interpolated by the Landmark software. These tended to be on the soft tissue menton and tragus of the ear area.

For some subjects that had faces landmarked, we did not include their basicrania in the data. Some of the basicrania thresholds that were used in the Amira software resulted in missing landmarks that were then interpolated by the Landmark software. These tended to be in the sella and internal occipital crest area.

Most clefts occur on the left side, so we did not have much data for the right side clefts. Unilateral cleft lip and cleft lip with palate show an approximately 2:1 bias toward left-sided clefts, meaning roughly two-thirds of unilateral cases occur on the left side (Gallagher 2018). We only had two individuals with clefts on the right side in the basicrania data set, and one individual with cleft on the right side in the face data set. This is why in studying asymmetry, we used the unilateral or bilateral category instead of distinguishing right side from left side.

When examining the relationship between cleft severity and cranial base morphology, as well as cleft severity and asymmetry of basicranium and face, our findings were quite limited due to not having many samples in each category of cleft type. Certain cleft types, such as unilateral cleft lip and palate, also occur more frequently than some more rare cleft types, such as isolated cleft palate, which limits how many data points per cleft type we could get. A larger sample size with more individuals per cleft type may be more conclusive.

Conclusion

This study demonstrates that measurable differences in cranial base and facial morphology exist between individuals with CL/P and unaffected controls, as captured by geometric morphometric analysis of CBCT images acquired at ages 7–11, prior to alveolar bone grafting or orthodontic intervention. These findings provide quantitative, three-dimensional support for the developmental framework in which the basicranium and face are morphologically integrated structures whose shapes covary in a systematic and predictable way.

Individuals with CL/P were found to have basicrania that are wider anteriorly and in the middle, narrower posteriorly, and shorter in the anterior-to-posterior dimension compared to non-cleft controls. Facially, the CL/P group exhibited smaller, less projecting midfaces that were wider. These basicranial and facial characteristics were concordant: wider anterior cranial bases were associated with wider, less projecting midfaces, consistent with the hypothesis that a broader forebrain early in development constrains the spatial positioning of the facial prominences and alters the timing and mechanics of facial prominence fusion.

Partial least squares analysis confirmed significant covariation between basicranial and facial shape. Non-cleft individuals tended toward narrower, longer, and more anteriorly projecting faces paired with correspondingly narrower and longer basicrania, while the opposite pattern characterized individuals with CL/P. This relationship held whether or not peripheral facial landmarks (ears, cheeks) were included, indicating that the core association is driven by midface and mouth-region morphology rather than artifact of landmark selection.

Cranial base flexure explained notably less variance than the cranial width measures, though still significant at $p < 0.05$. While trends toward greater basicranial and facial asymmetry were observed in the CL/P group, the relationship between cleft severity and asymmetry did not reach statistical significance, likely owing to limited subgroup sample sizes. No clear relationship between cleft severity and specific cranial base or facial morphometric parameters was established, though the aggregate cleft-versus-noncleft contrasts were strong.

Clinical Significance and Implications

These findings have several practical implications for the clinical management of CL/P. Because the basicranial shape parameters captured at the pre-ABG time point represent a relatively stable developmental baseline — the midline basicranium approaches adult-like maturity at approximately 7–8 years — a wider anterior cranial base or shorter basicranial length identified at this age may serve as an early marker for a less projecting, wider midface later in development.

The CL/P basicranial morphological profile — wide anteriorly, narrow posteriorly, short in length — may be associated with the skeletal Class III pattern common in CL/P, and early recognition of this pattern could allow orthodontists to anticipate significant anteroposterior discrepancy and initiate interceptive treatment, such as maxillary protraction, at the optimal time. Similarly, awareness of this basicranial pattern may help surgical teams counsel families earlier about the likelihood of future orthognathic intervention.

The trend toward greater asymmetry in the presence of unilateral CL/P is also clinically relevant, despite limited results relating asymmetry and cleft severity. Basicranial asymmetry may be a primary contributor to the facial asymmetry observed in these patients, rather than a secondary consequence of the cleft or its repair. If confirmed in larger studies, this would support including basicranial asymmetry assessment in pre-surgical workups, helping clinicians set more realistic goals and patient expectations for procedures aimed at improving facial symmetry.

Future Directions

Longitudinal studies tracking the same individuals from the pre-ABG time point through skeletal maturity are needed to determine whether early basicranial shape predicts adult facial outcomes and the need for orthognathic surgery. Larger samples with sufficient representation of each cleft type will be necessary to determine whether cleft severity is independently associated with specific morphological parameters. Expanding landmark protocols to include finer basicranial structures and incorporating automated landmarking methods to reduce inter-rater variability and improve scalability could be important next steps. Together, these could help basicranial geometric morphometrics become a practical and informative tool for the craniofacial team's clinical assessment.

Figures and Tables

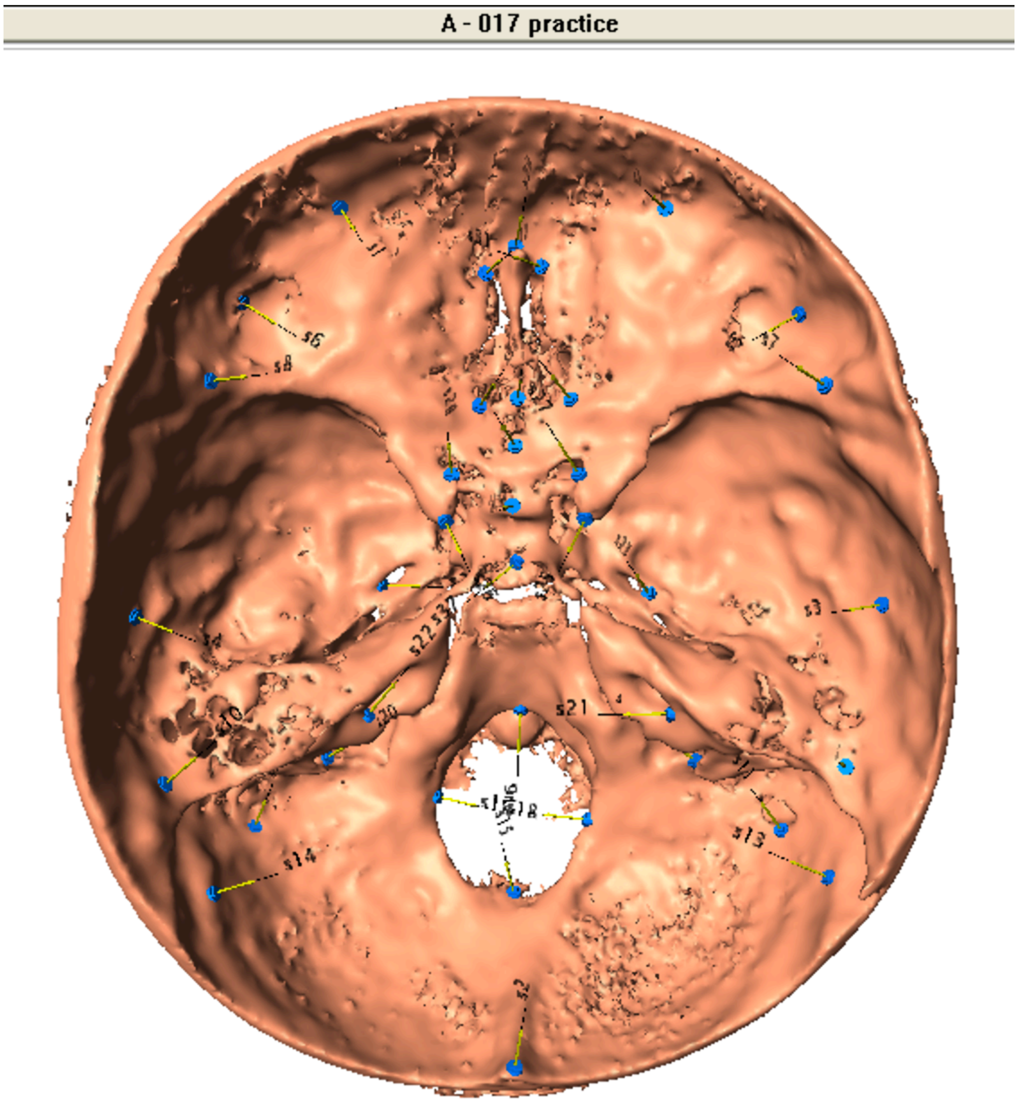

Figure 1: *Example of landmarked basicranium*

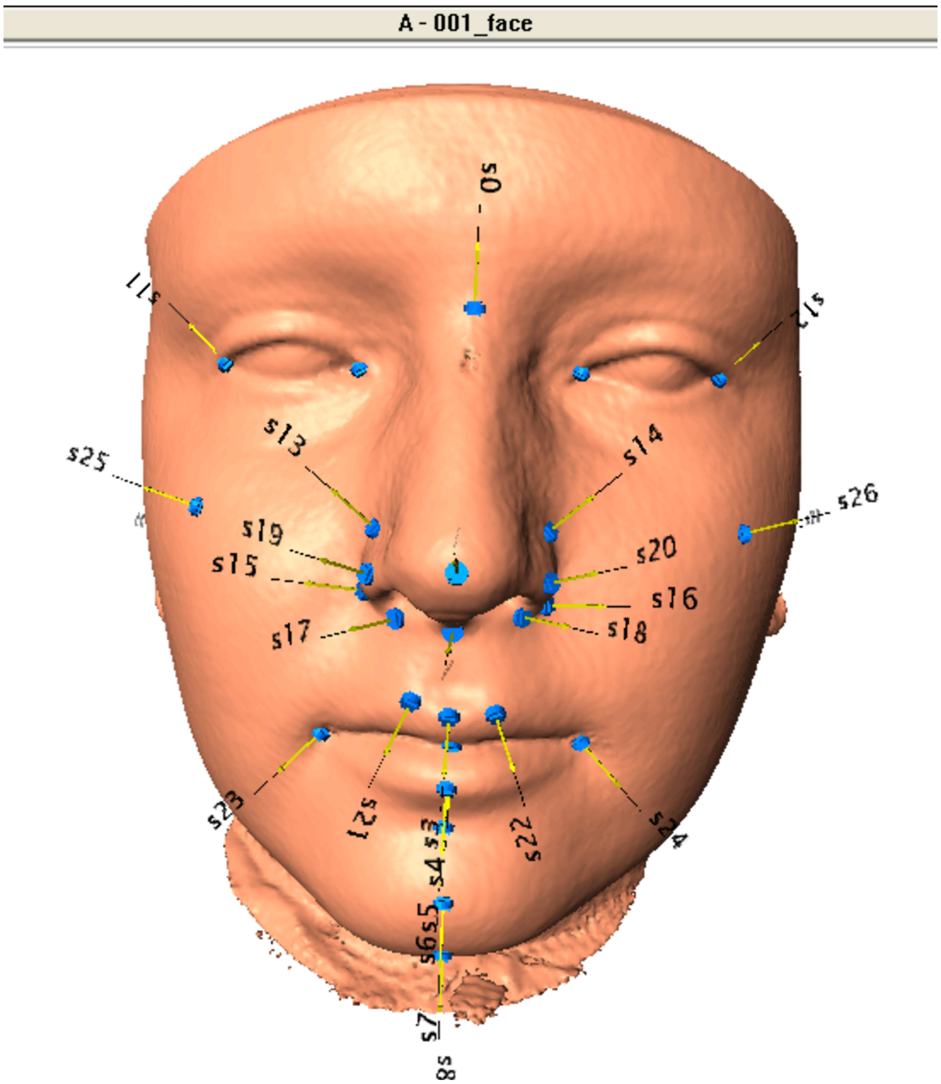

Figure 2: *Example of landmarked face*

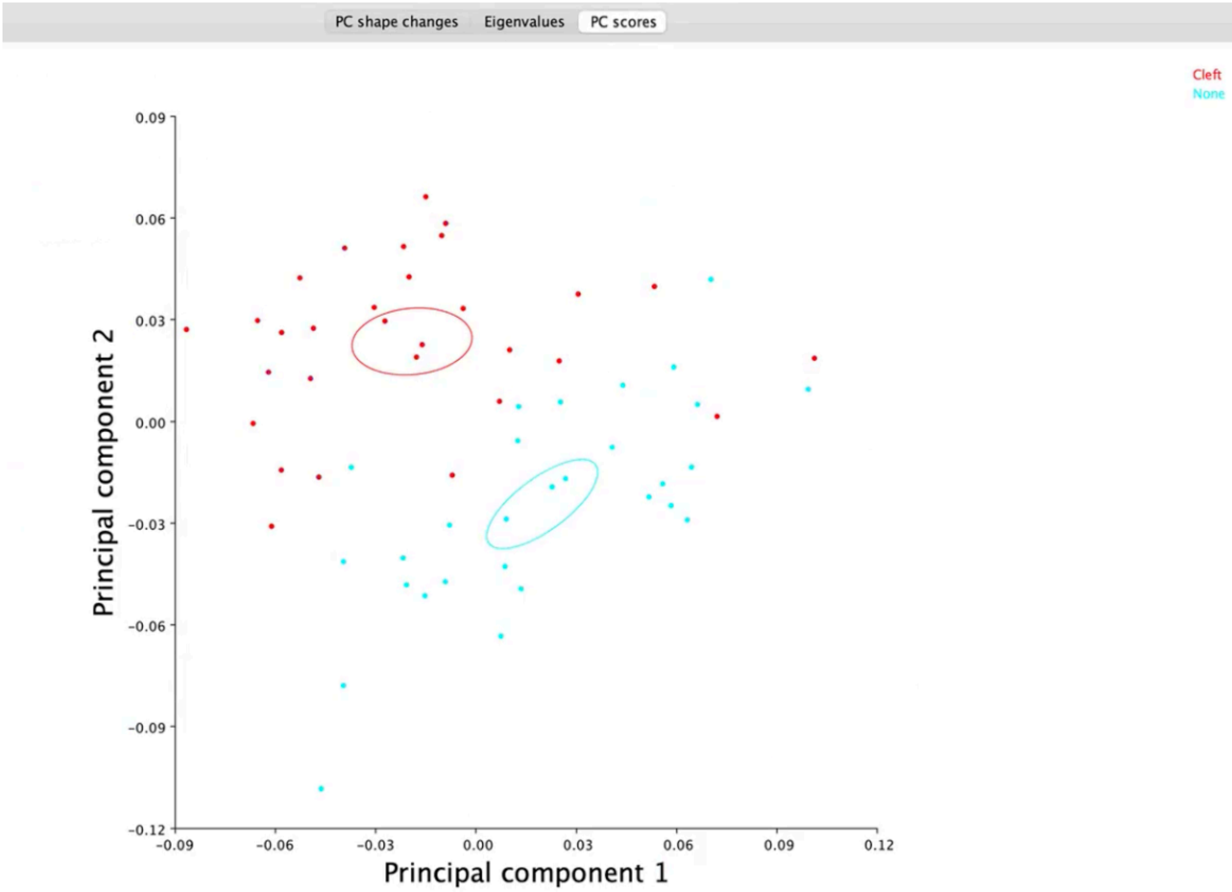

Figure 3: *PC scores of cleft vs. non-cleft basicrania*

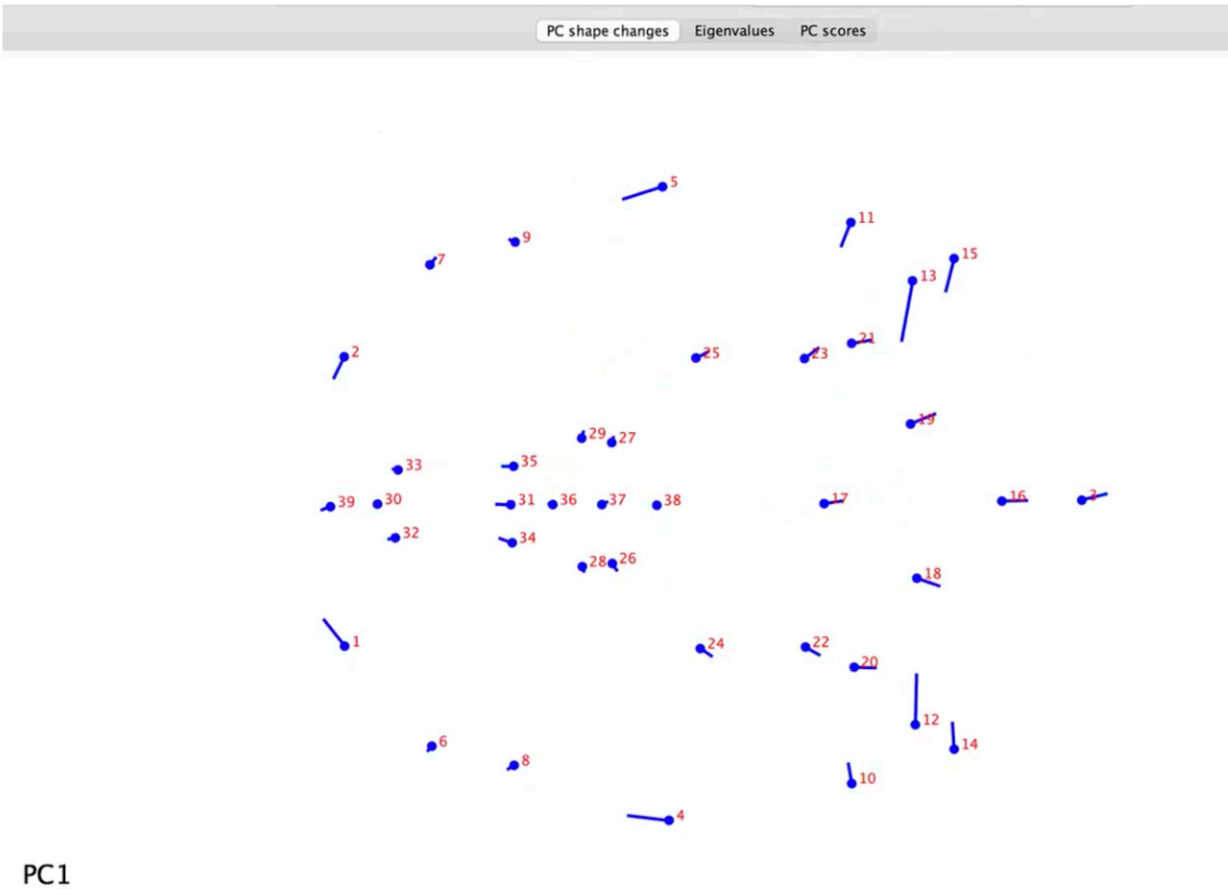

Figure 4: *PC1 shape changes for cleft vs non-cleft basicrania*

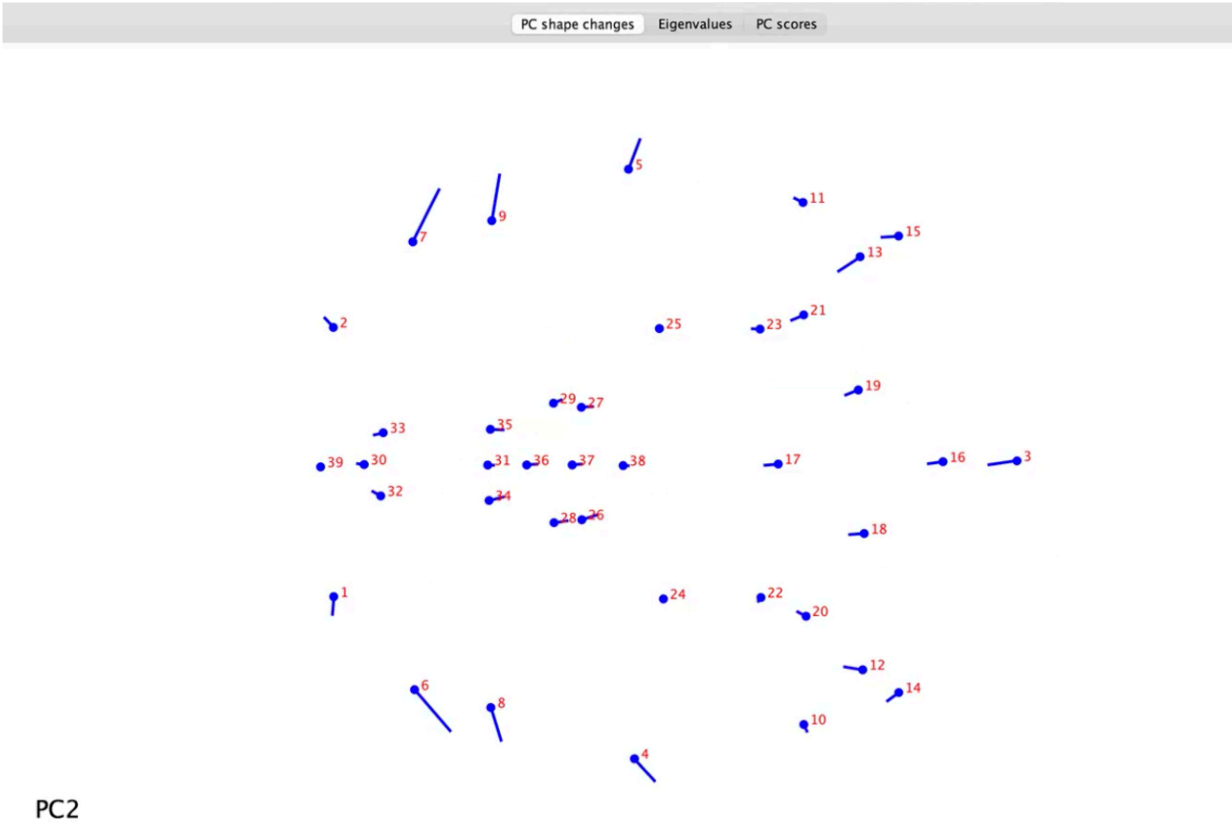

Figure 5: *PC2 shape changes for cleft vs. non-cleft basicrania*

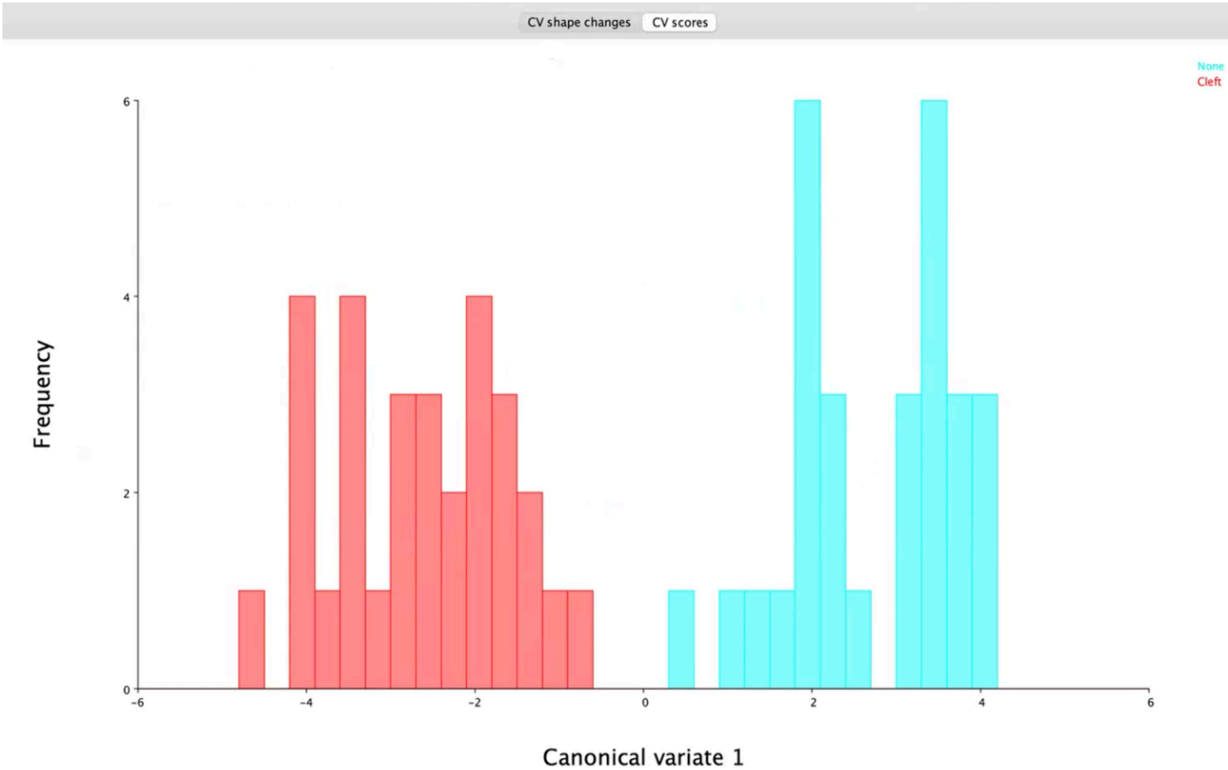

Figure 6: *CV scores bar graph for cleft vs. non-cleft basicrania*

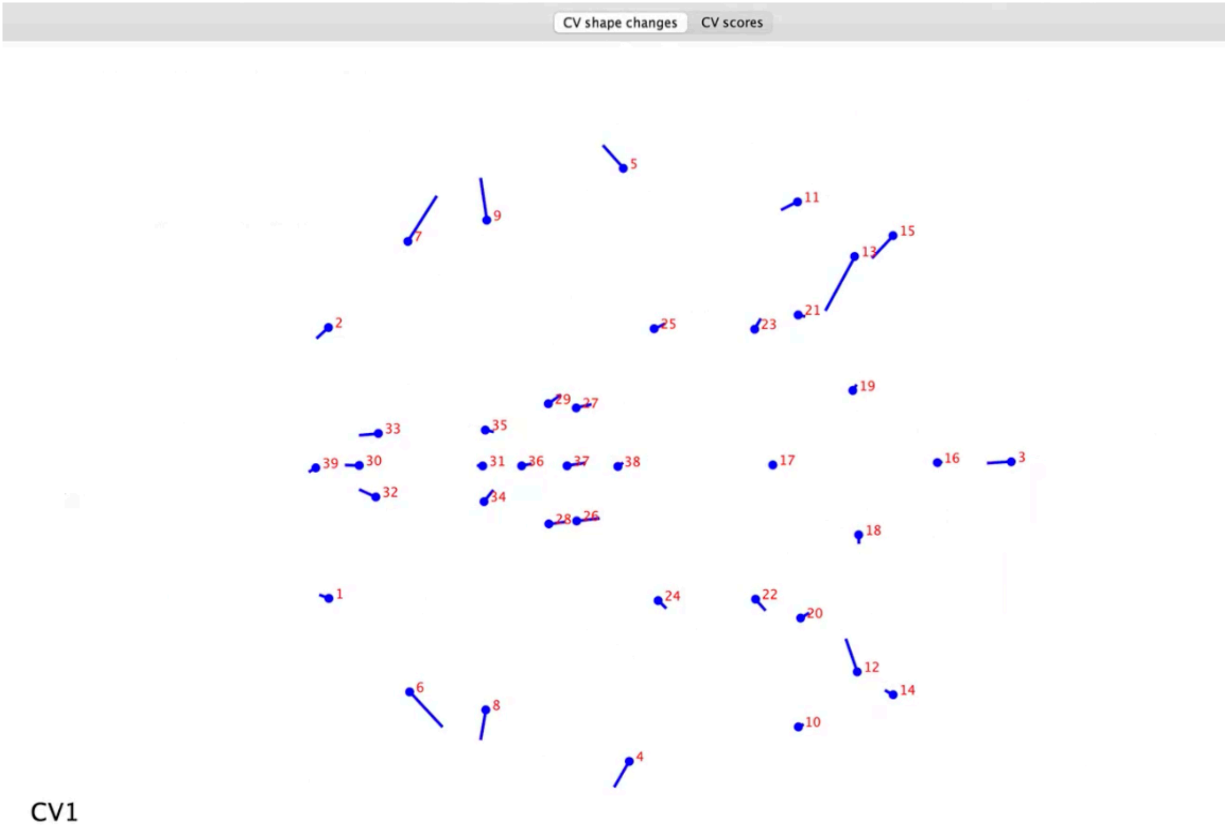

Figure 7*: CV shape changes for cleft vs. non-cleft basicrania*

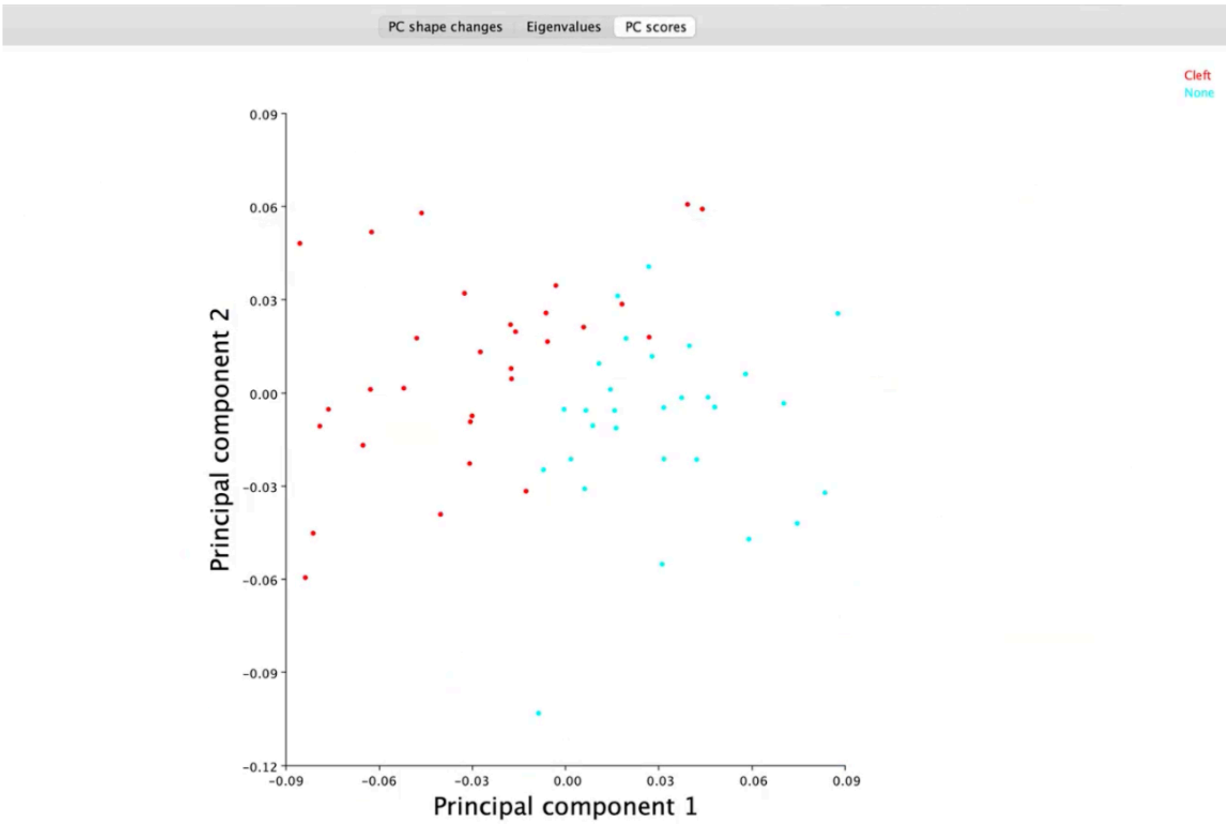

Figure 8: *PC scores of cleft vs. non-cleft faces*

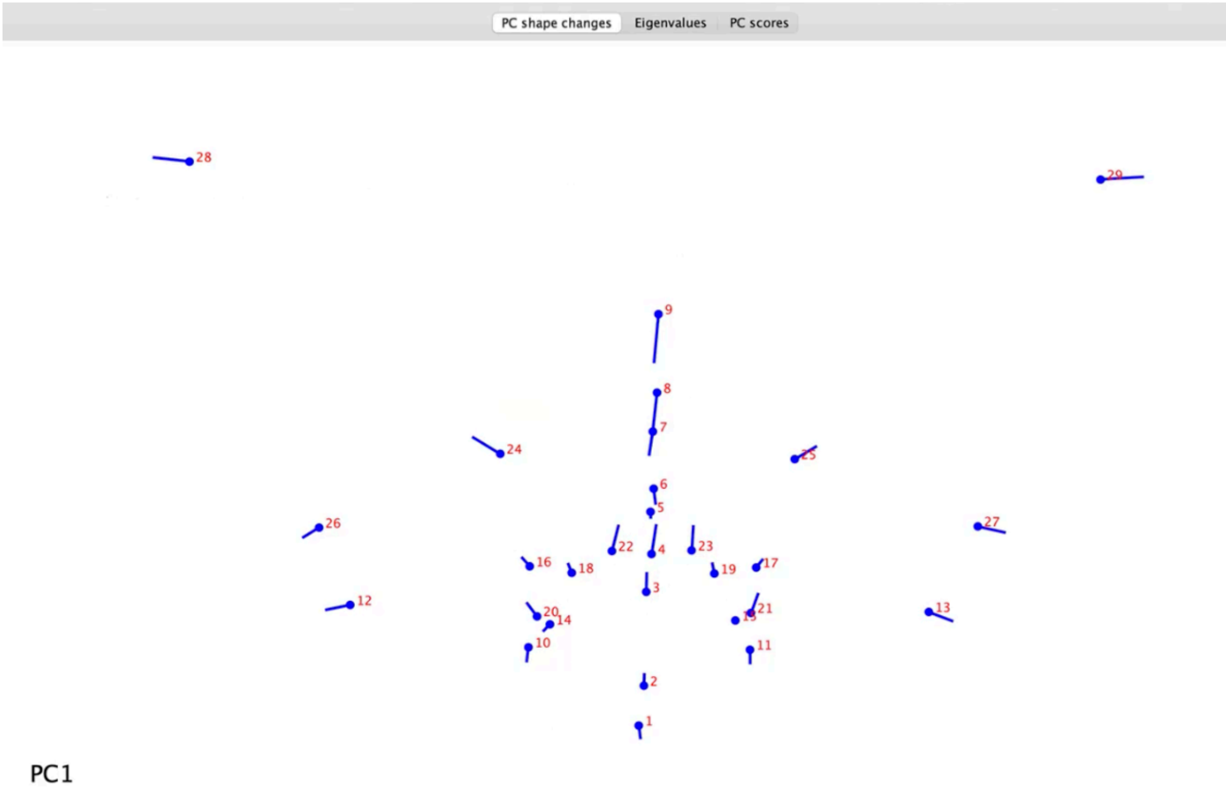

Figure 9: *PC1 shape changes for cleft vs. non-cleft faces*

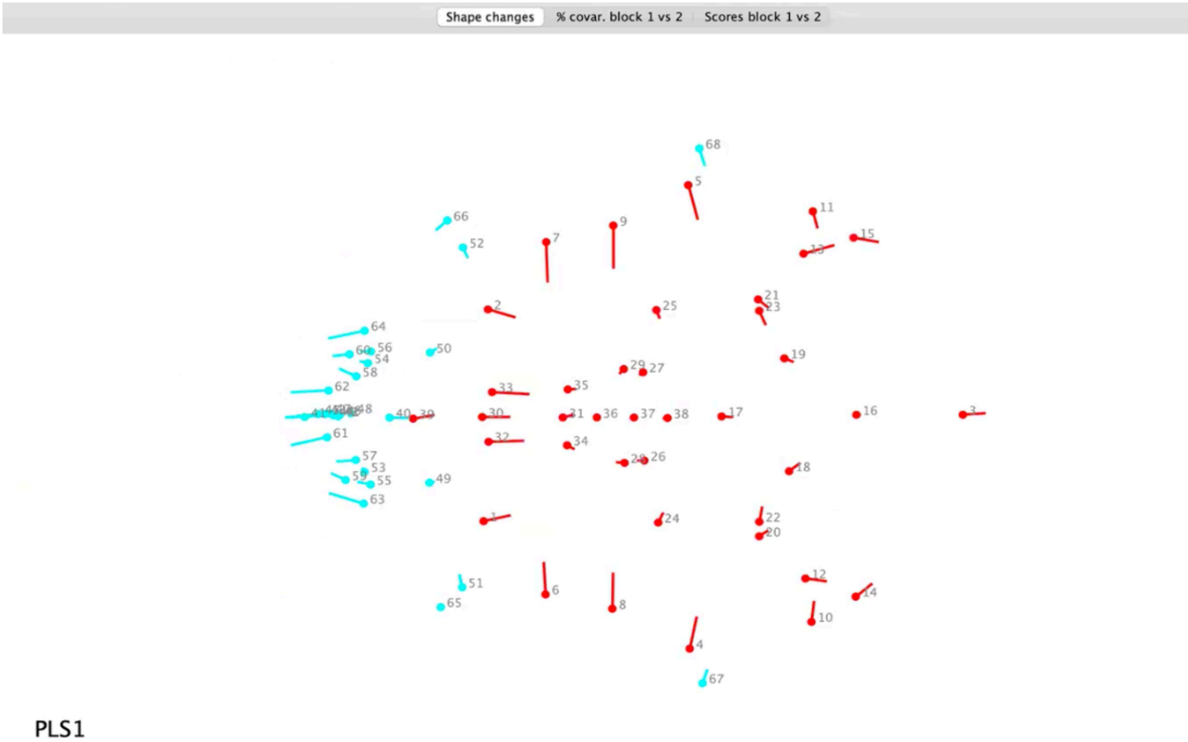

Figure 10: *PLS shape changes of basicrania and faces*

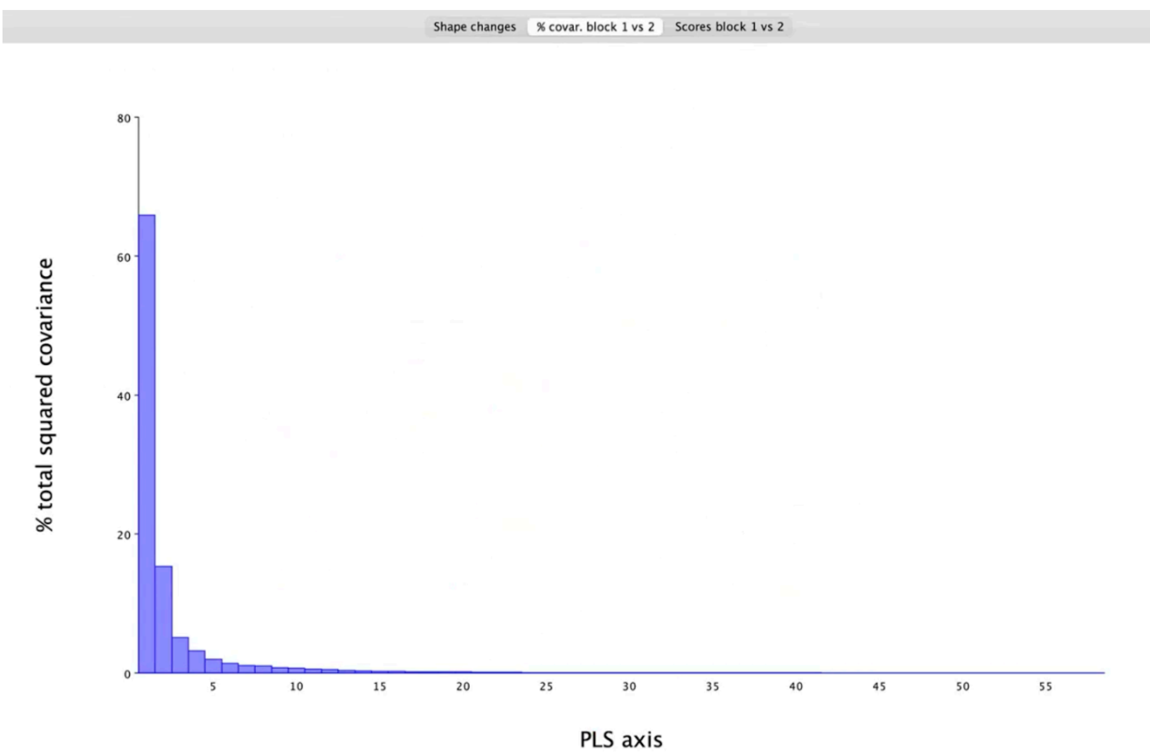

Figure 11: *PLS axis*

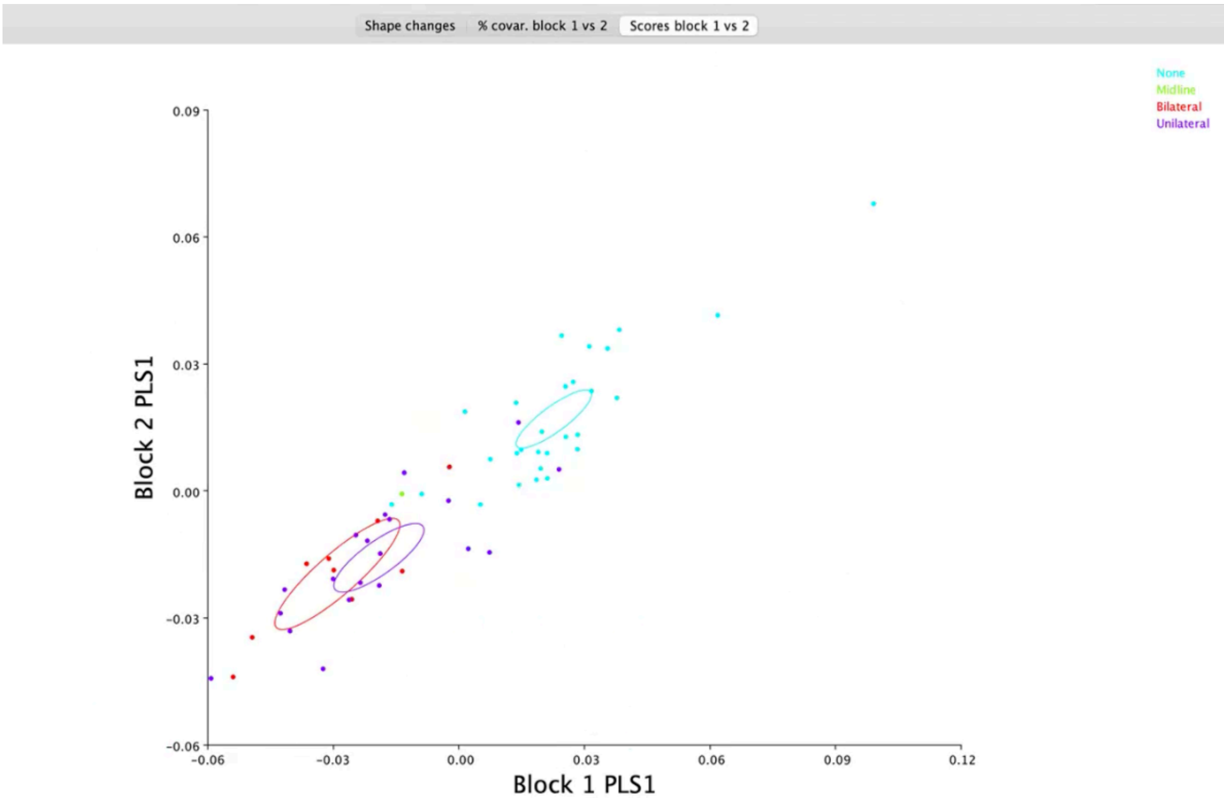

Figure 12: *Scores along PLS1 for each block*

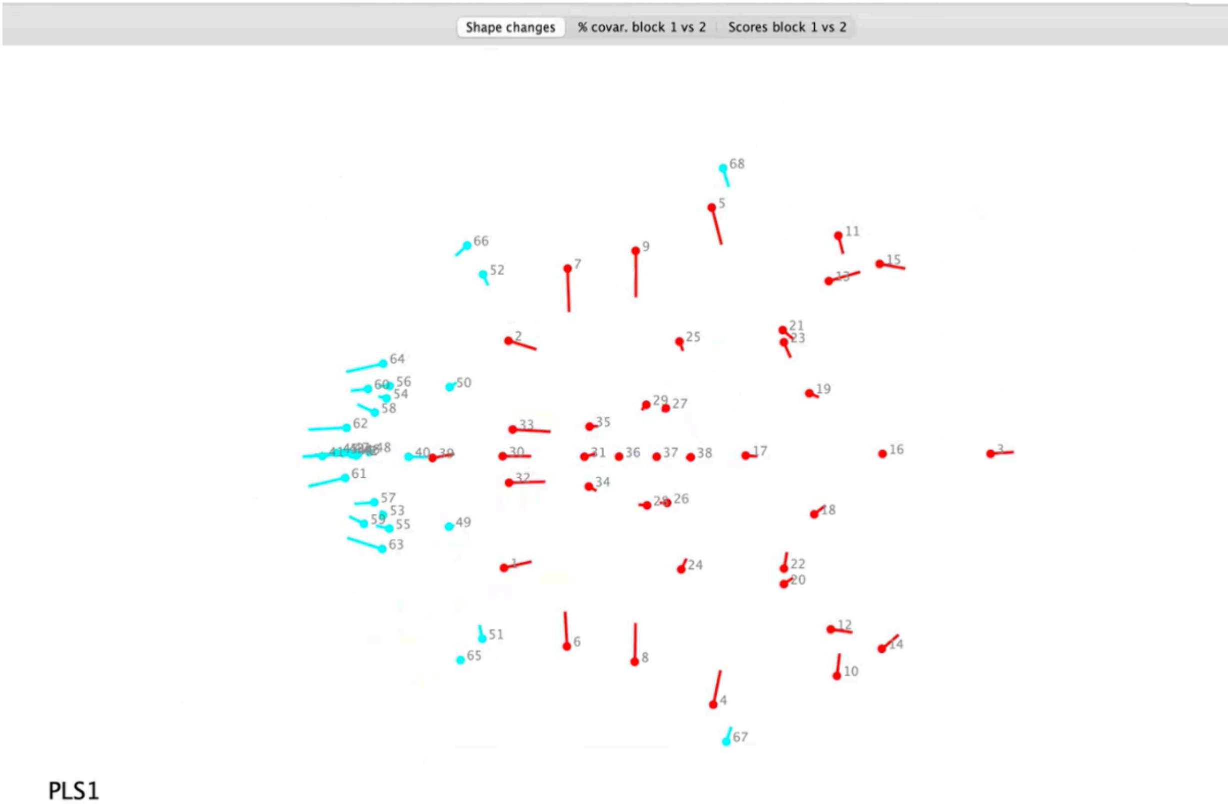

Figure 13: *PLS1 shape changes for positive scores*

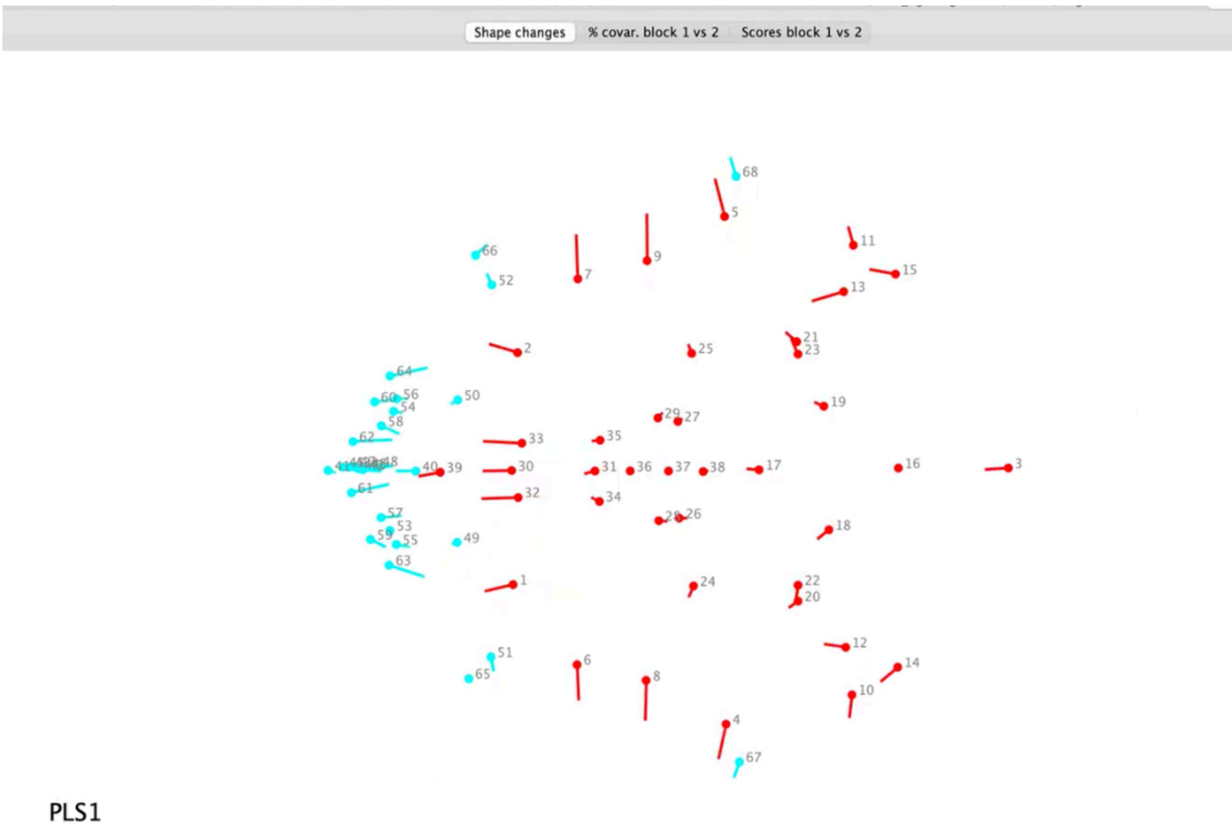

Figure 14: *PLS1 shape changes for negative scores*

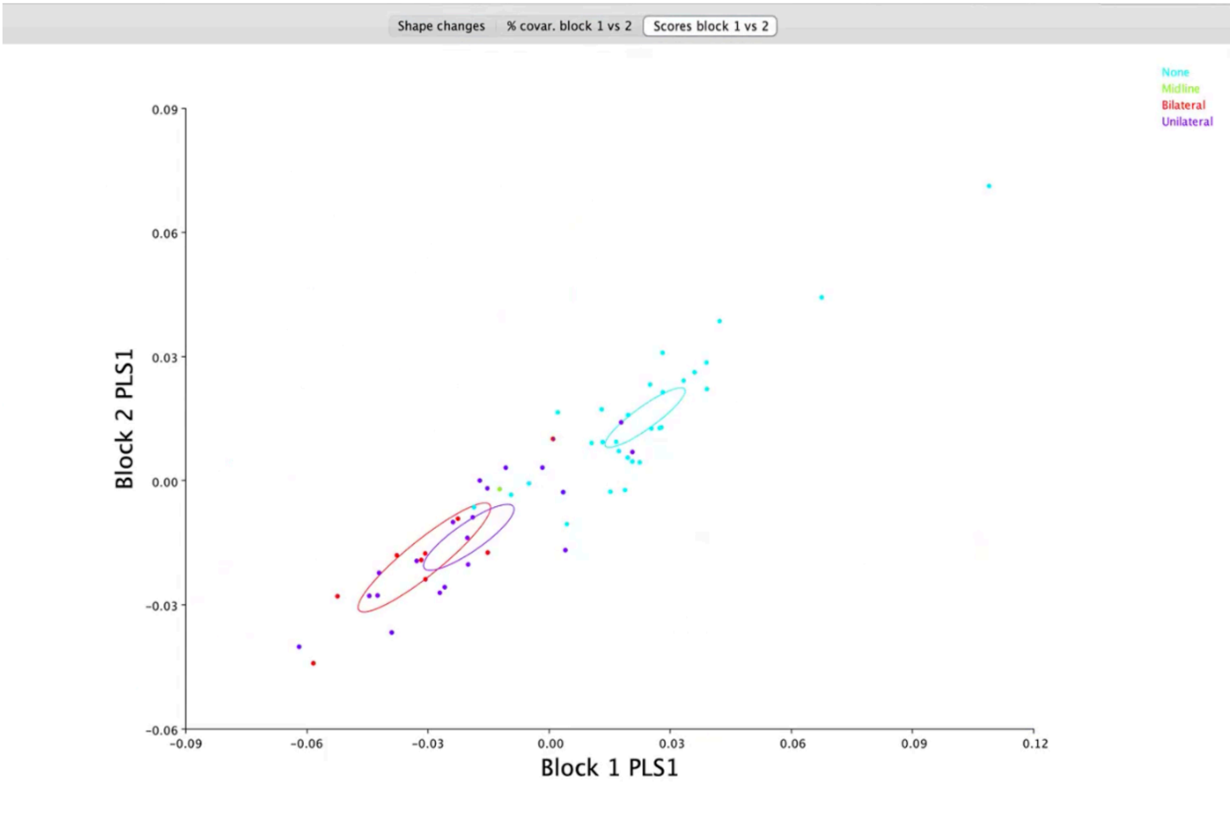

Figure 15: *Scores along PLS1 for landmarks on midface and mouth area*

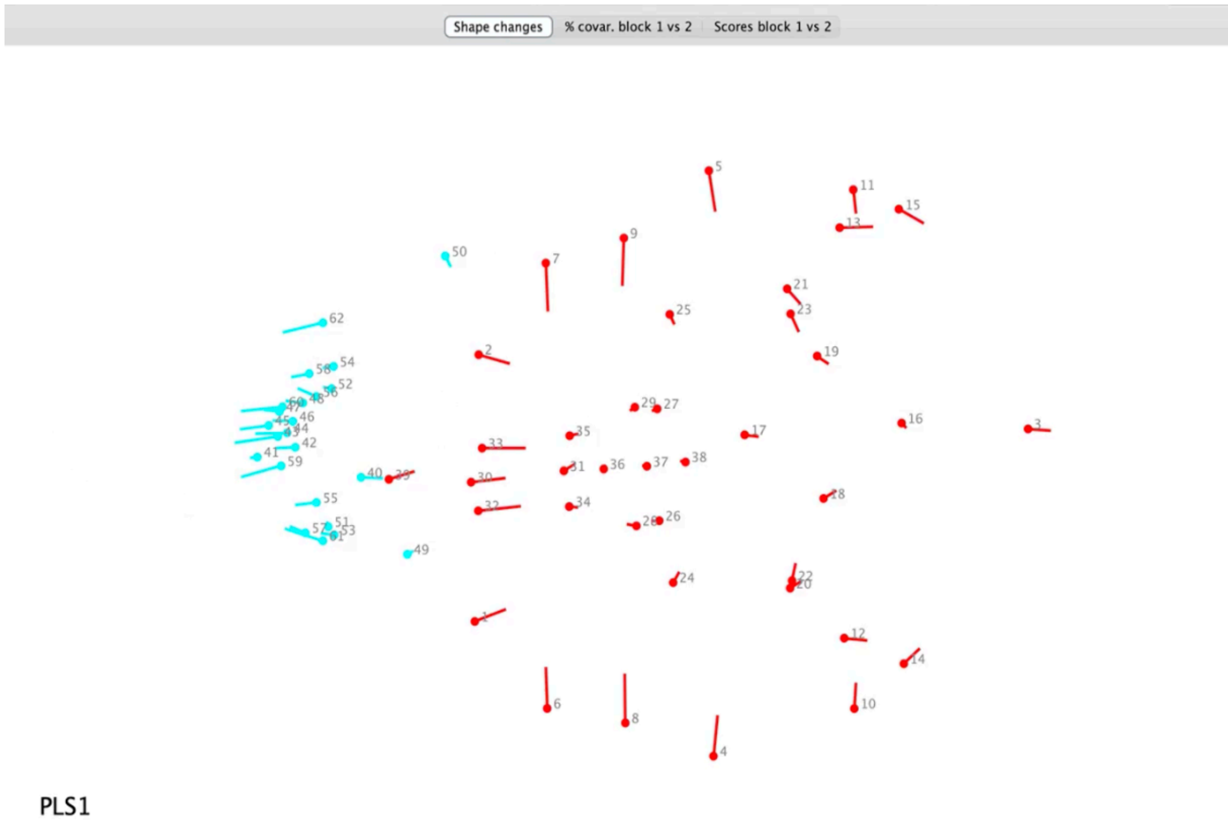

Figure 16: *PLS1 shape changes for positive scores for landmarks on midface and mouth area*

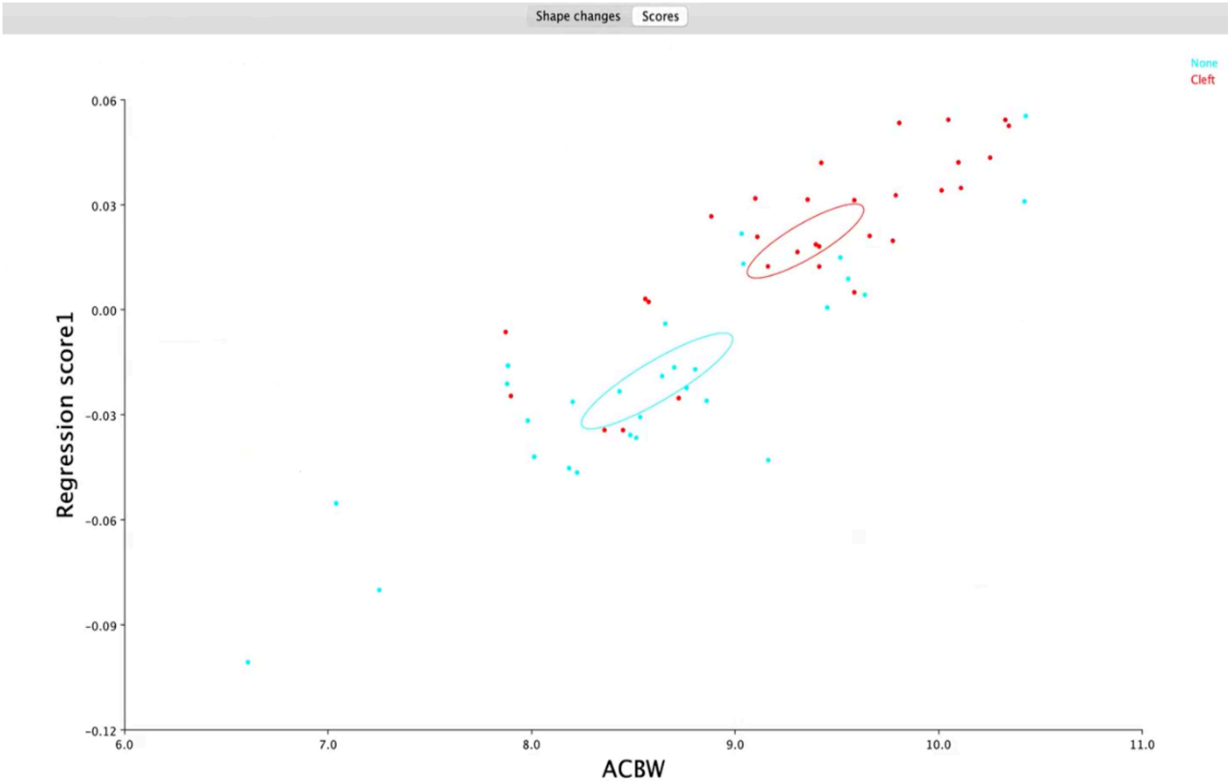

Figure 17: *Regression of basicranium with anterior cranial base width*

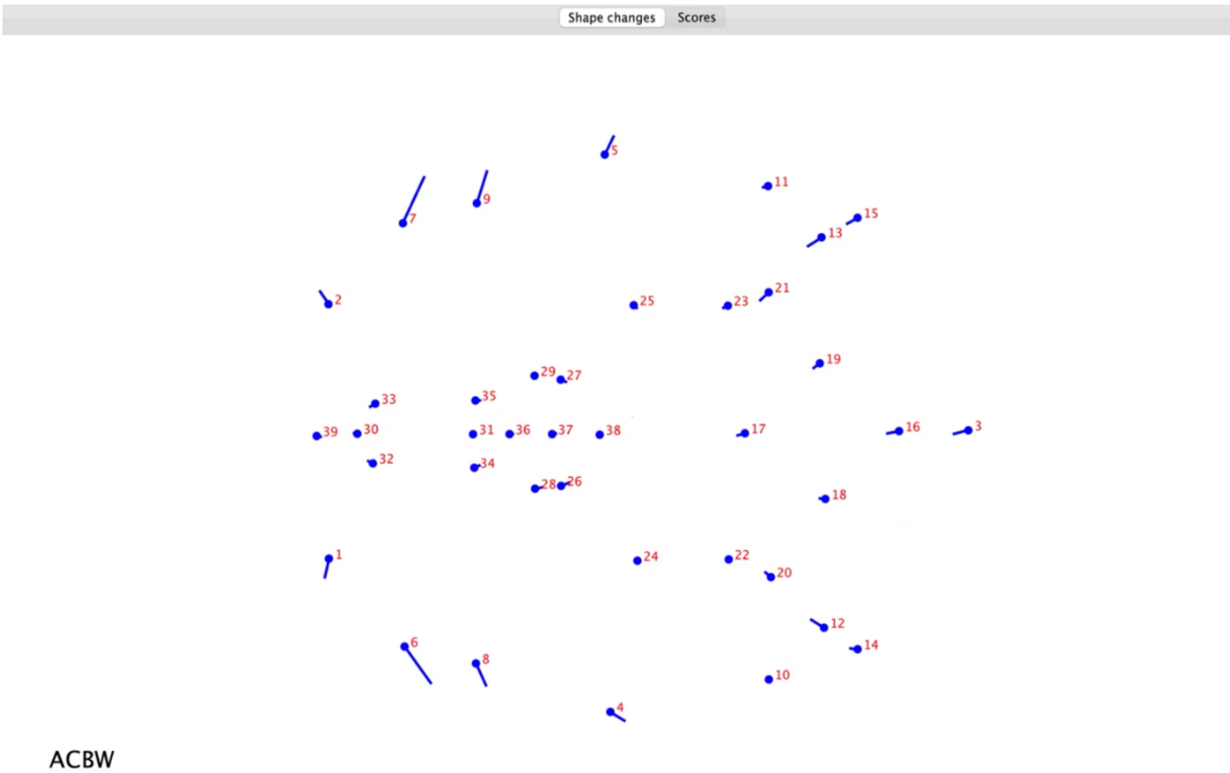

Figure 18: *Shape changes of regression of basicranium with anterior cranial base width*

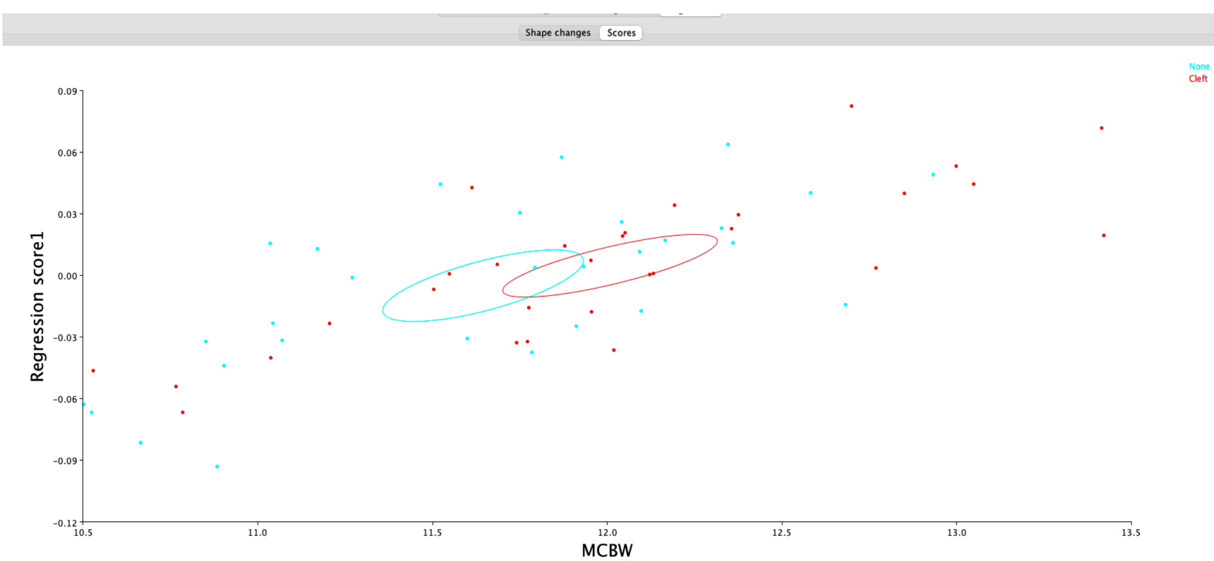

Figure 19: *Regression of basicranium with middle cranial base width*

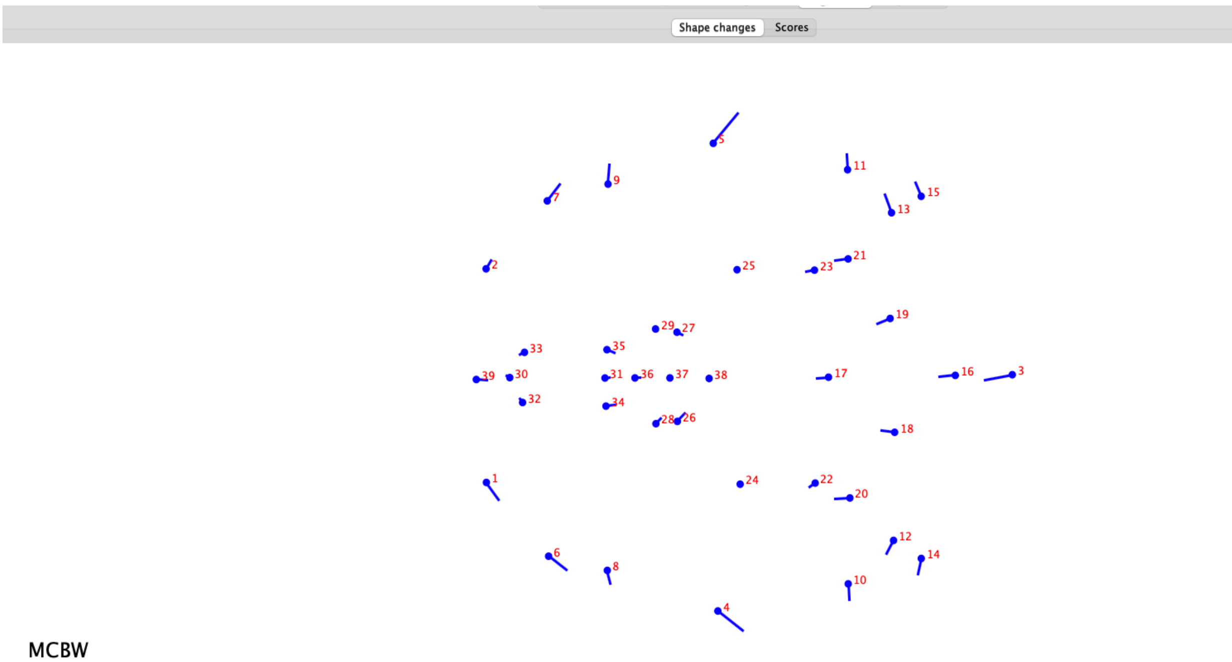

***Figure 20**: Shape changes of regression of basicranium with middle cranial base width*

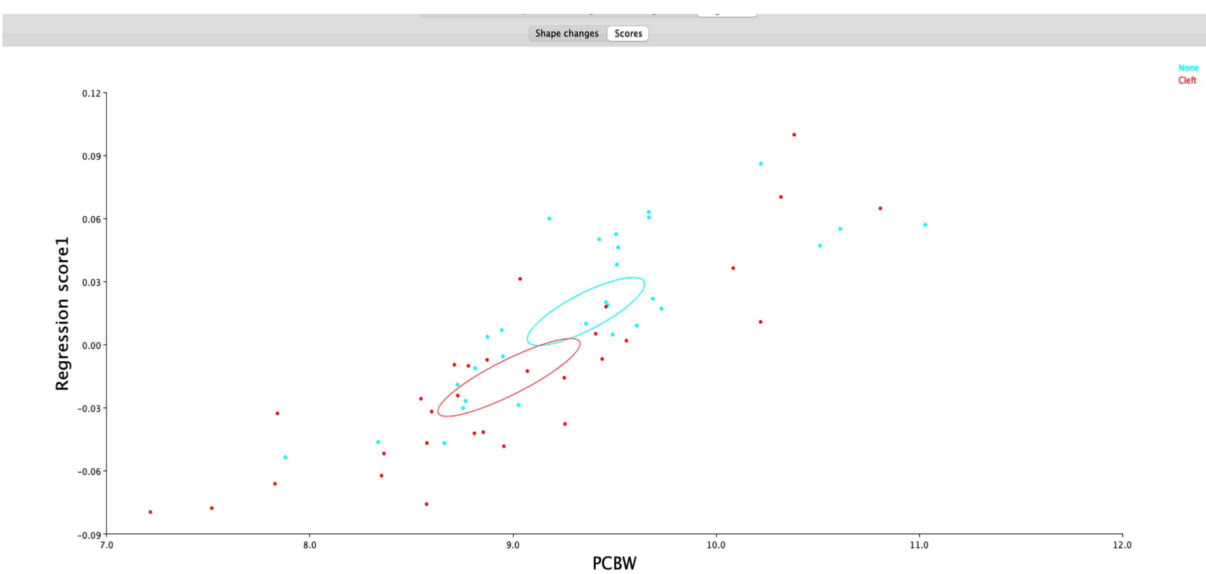

***Figure 21**: Regression of basicranium with posterior cranial base width*

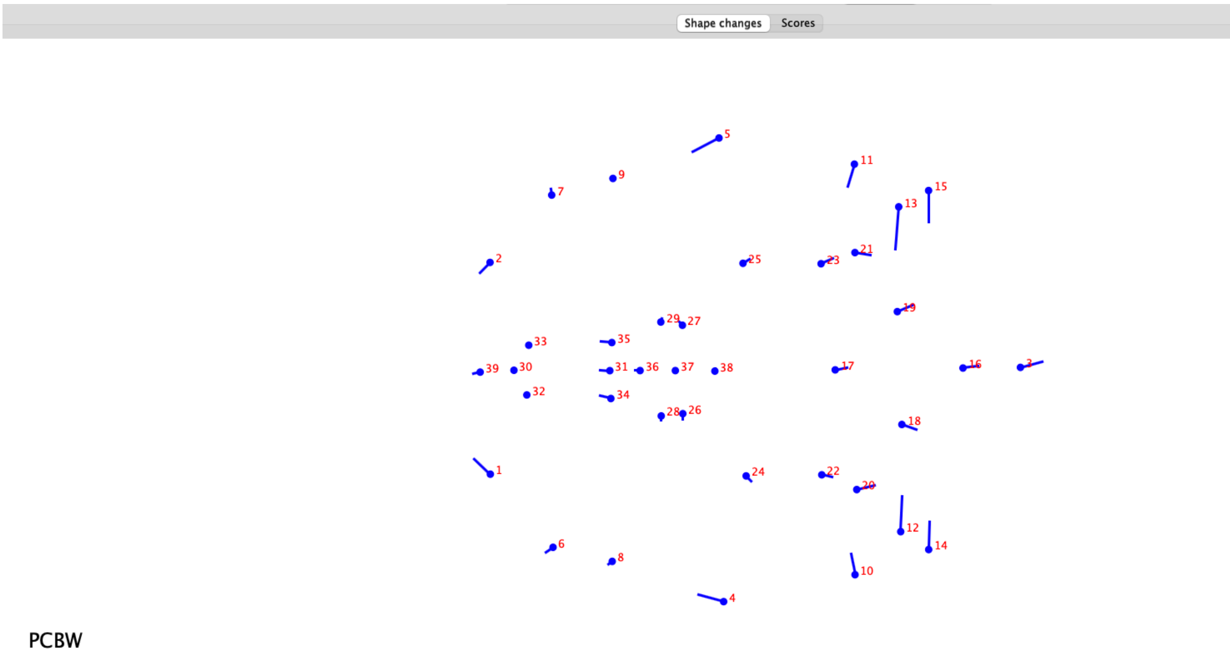

Figure 22*: Shape changes of regression of basicranium with posterior cranial base width*

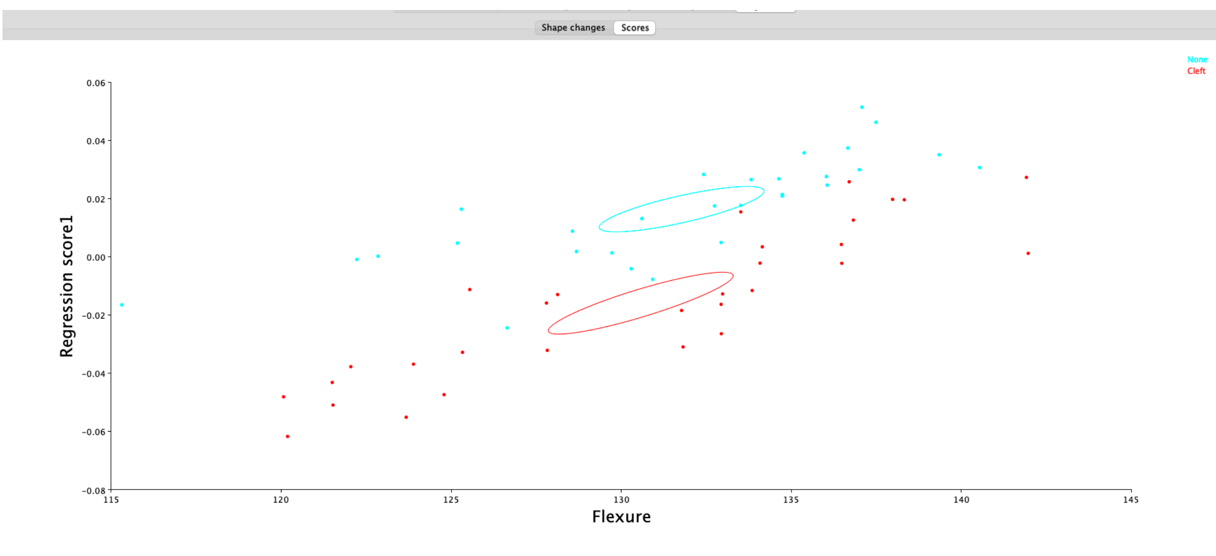

Figure 23: *Regression of basicranium with flexure of cranial base (SN-Basion angle)*

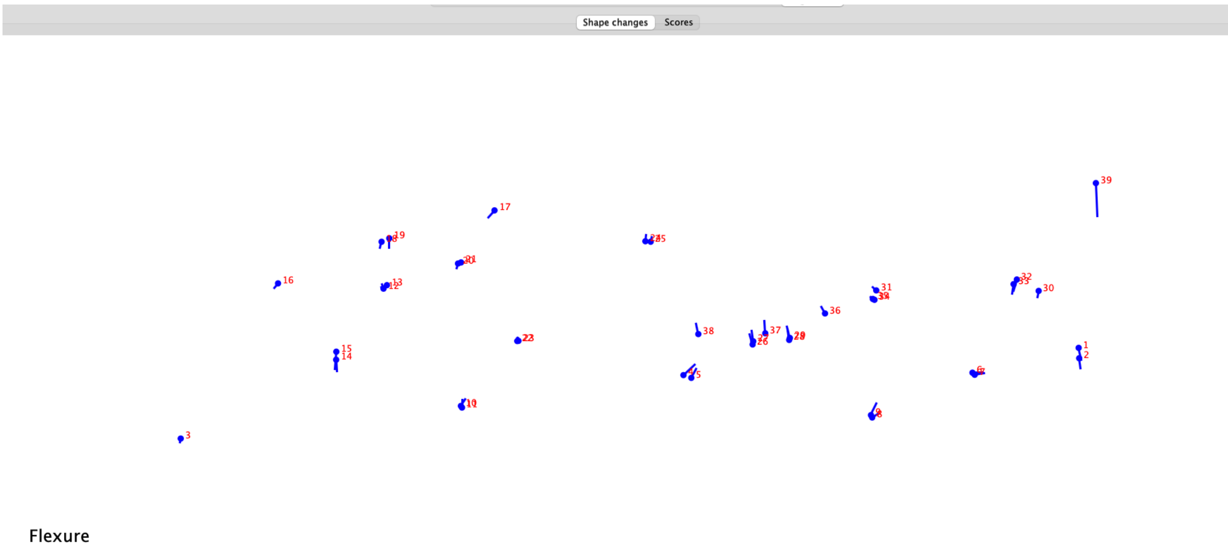

Figure 24: *Shape changes of regression of basicranium with flexure of cranial base (SN-Basion angle)*

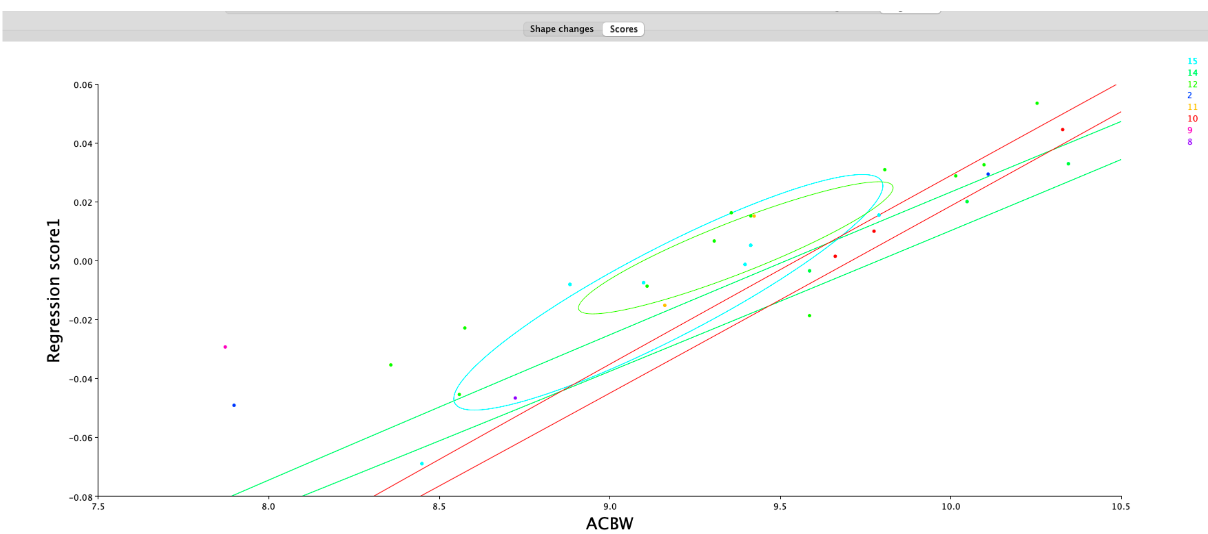

Figure 25: *Regression of cleft basicranium with anterior cranial base width by cleft severity*

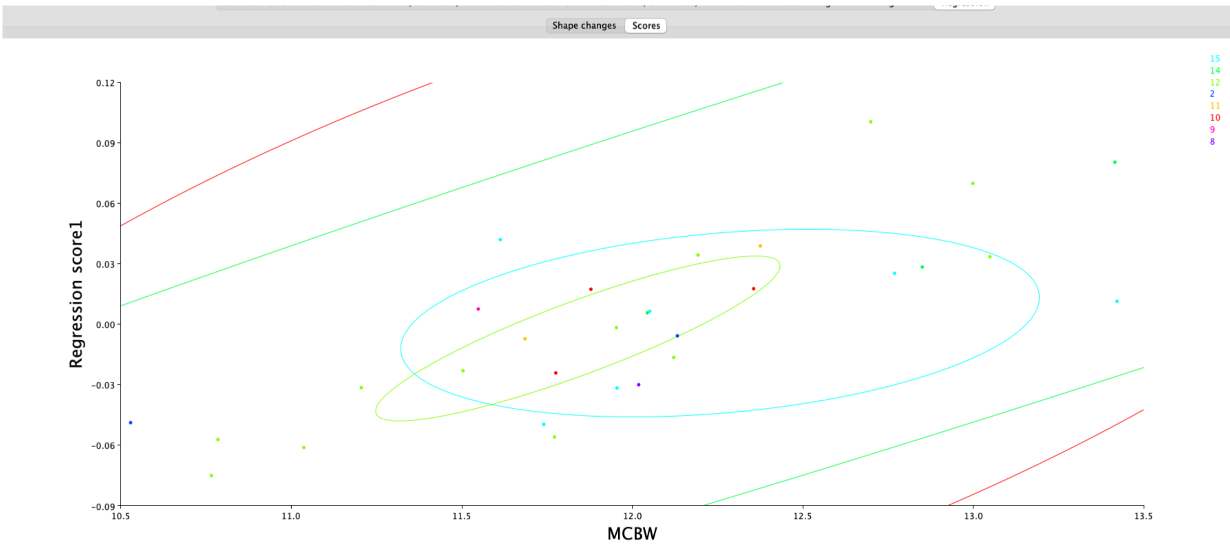

Figure 26: *Regression of cleft basicranium with middle cranial base width by cleft severity*

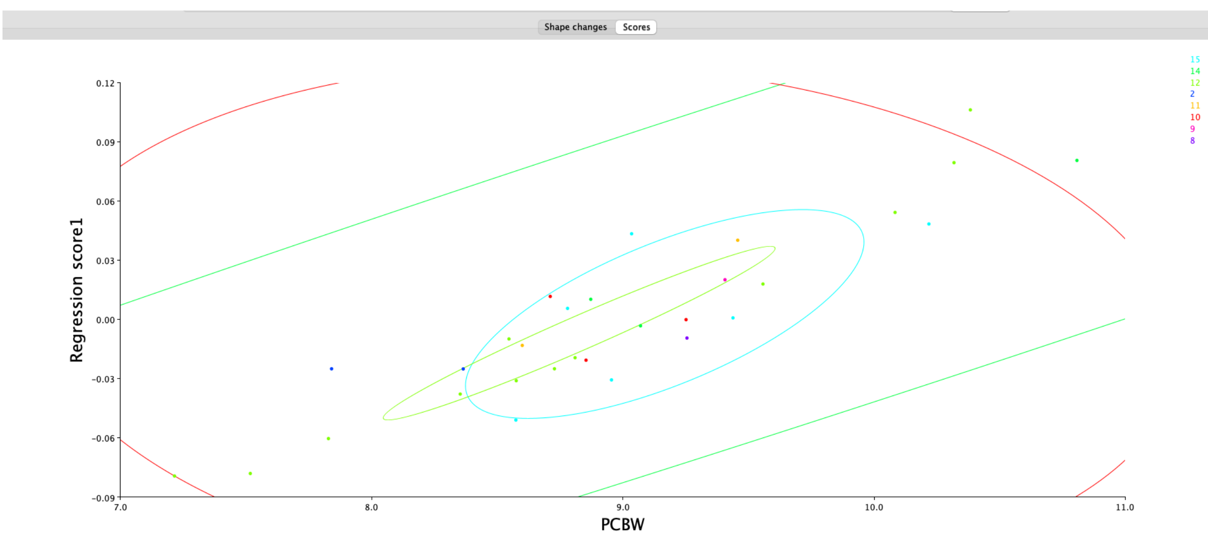

Figure 27: *Regression of cleft basicranium with posterior cranial base width by cleft severity*

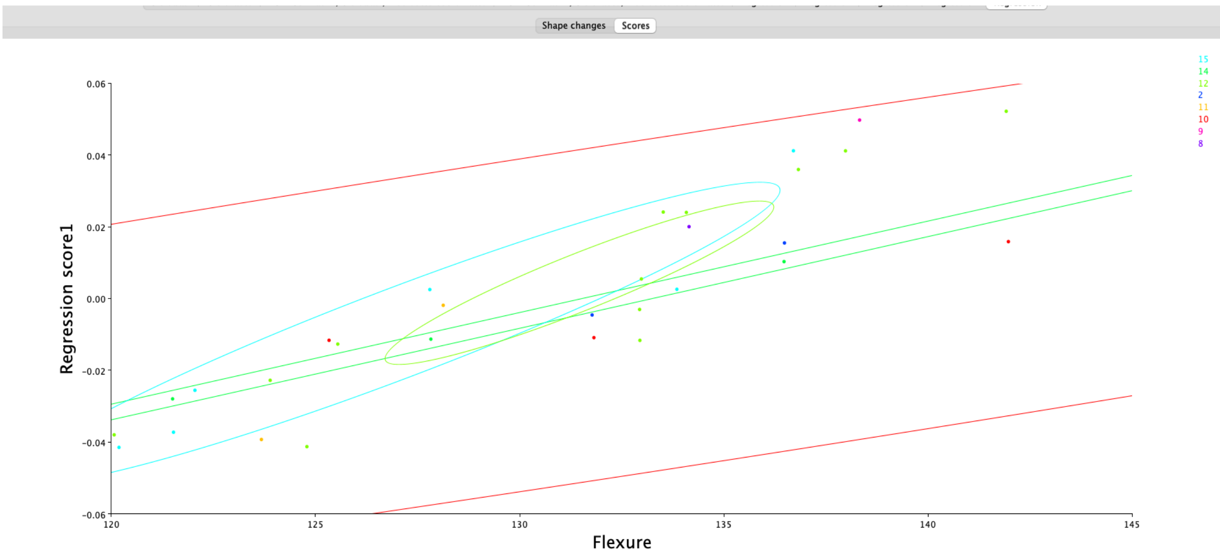

Figure 28: *Regression of cleft basicranium with flexure of cranial base (SN-Basion angle) by cleft severity*

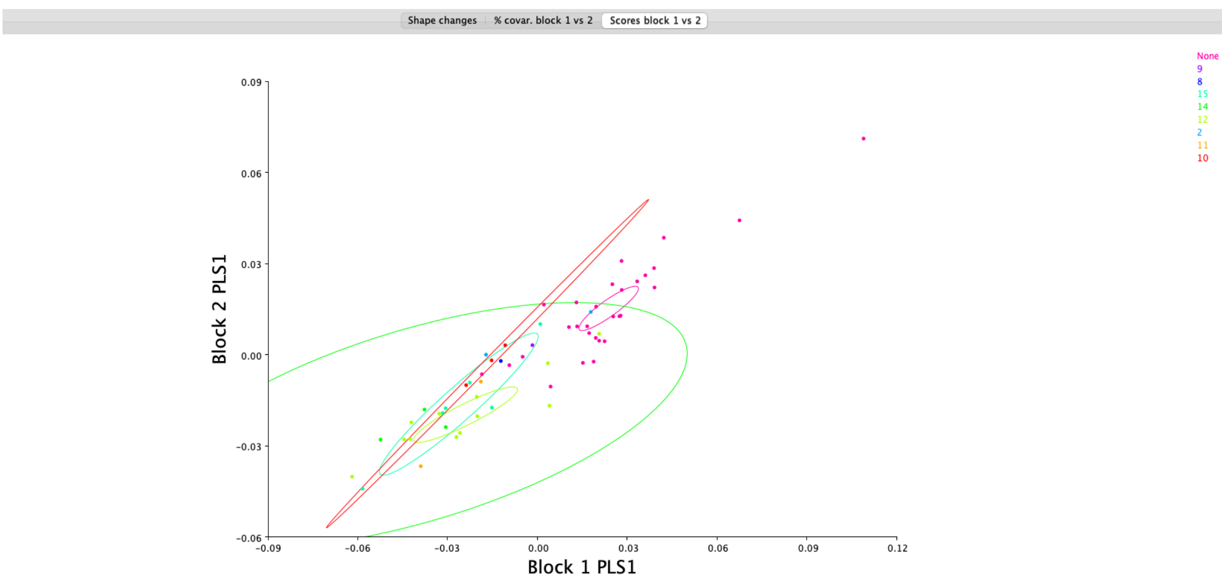

Figure 29: *Scores along PLS1 for each block, colored by cleft severity*

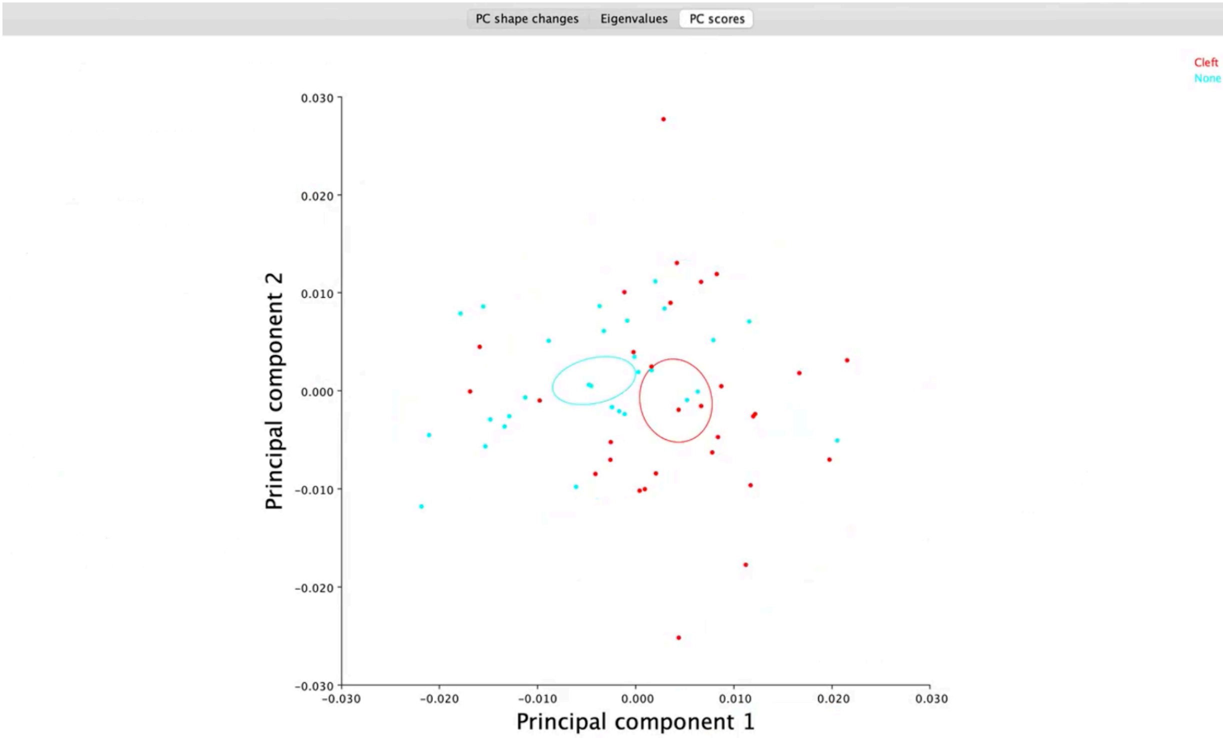

Figure 30: *PC scores of asymmetric shape component by presence of cleft*

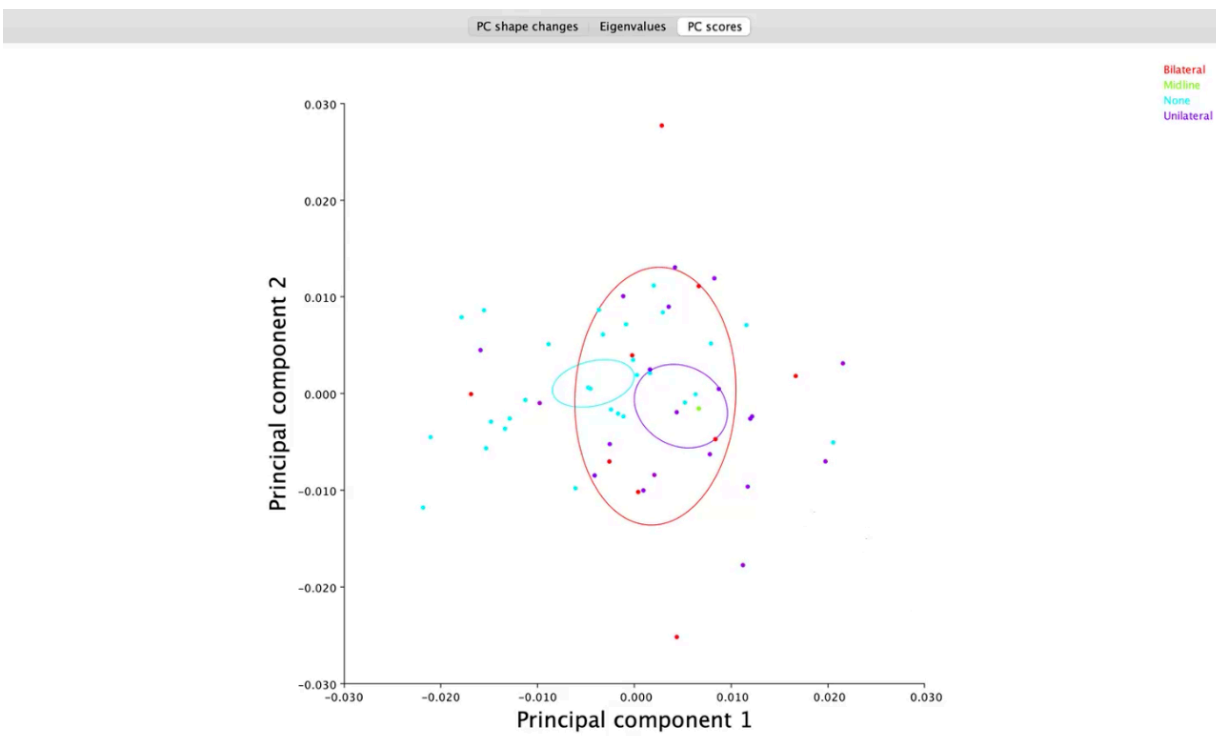

Figure 31: *PC scores of asymmetric shape component by laterality of cleft*

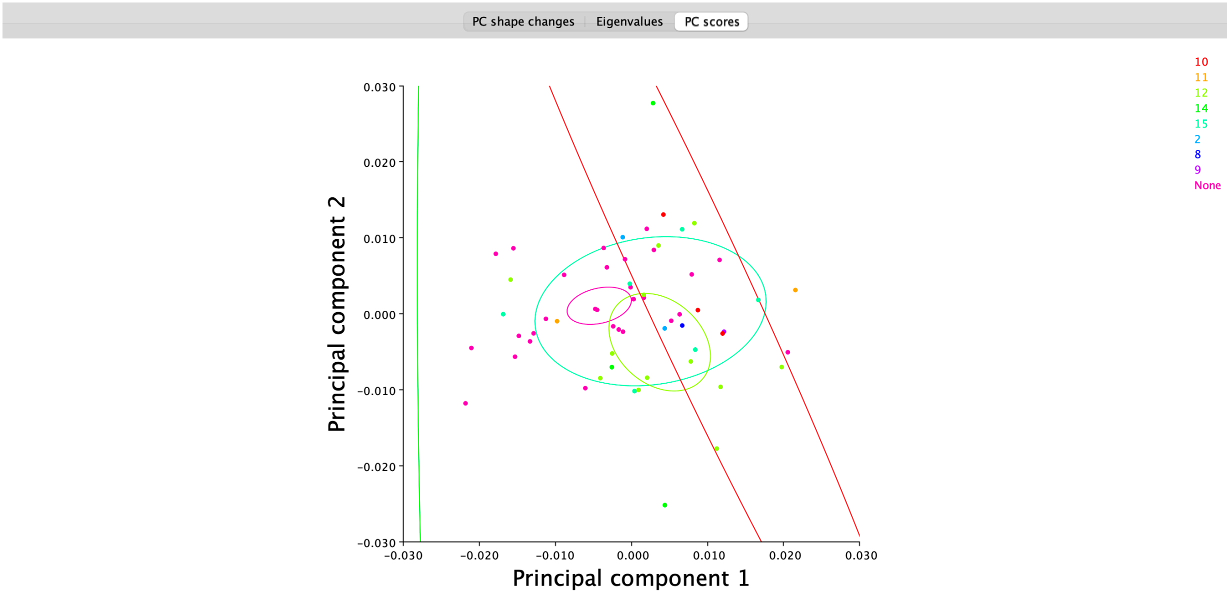

Figure 32: *PC scores of asymmetric shape component by cleft severity*

Table 1: *Severity of cleft type ranked by number*

Rank number	Type of cleft
1	Microform Cleft Lip (forme fruste)
	A minimal, often cosmetic indentation or scar-like mark on the lip. No real cleft; muscles may or may not be involved.
2	Incomplete Unilateral Cleft Lip
	Partial cleft on one side of the upper lip. Does **not** extend into the nostril.
3	Complete Unilateral Cleft Lip
	Full cleft on one side, extending up into the nostril. May affect the underlying muscle and nasal structure.
4	Incomplete Bilateral Cleft Lip
	Partial clefts on both sides of the upper lip. Clefts do **not** reach the nostrils.
5	Complete Bilateral Cleft Lip
	Full clefts on both sides of the lip, extending into both nostrils. The philtral tissue (central lip) may be isolated as a "prolabium."
6	Isolated Submucous Cleft Palate
	Palate appears intact but has underlying muscular separation. Includes signs like bifid uvula, zona pellucida, or velopharyngeal insufficiency.
7	Isolated Cleft of Soft Palate

Rank number	Type of cleft
	Only the soft palate (posterior part) is cleft. Speech and feeding may be affected.
8	Isolated Cleft of Hard and Soft Palate
	Cleft involves both hard and soft palate, but no cleft lip. Midline defect due to failed fusion of palatal shelves.
9	Unilateral incomplete Cleft Lip and Alveolus
	Involves the lip and extends into the gum ridge (alveolus) on one side.
10	Unilateral complete cleft lip and alveolus
11	Unilateral incomplete cleft lip and palate
12	Unilateral Complete Cleft Lip and Palate
	Cleft involves lip, alveolus, and continues into the palate (both hard and soft), on one side.
13	Bilateral Cleft Lip and Alveolus
	Both sides of lip and gum ridge involved, but palate may be intact.
14	Bilateral CL/P, complete CLP on one side and cleft lip or incomplete CLP on the other
15	Bilateral Complete Cleft Lip and Palate
	Most severe form. Full clefts on both sides of lip, alveolus, and palate (hard and soft). Prolabium (central lip portion) is often unattached.

Table 2: *List of basicrania landmarks*

Landmark #	Name of Landmark	Description
1	R anterior cranial base (antero-lateral)	Most anterior and lateral point of the anterior cranial base (R side)
2	L anterior cranial base (antero-lateral)	Most anterior and lateral point of the anterior cranial base (L side)
3	Internal occipital crest	Most posterior, superior midline point of internal occipital crest
4	R squamous part of temporal bone	Most lateral point of squamous part of temporal bone (R side)
5	L squamous part of temporal bone	Most lateral point of squamous part of temporal bone (L side)
6	R anterior cranial base (lateral)	Most lateral point of anterior cranial base (R side)
7	L anterior cranial base (lateral)	Most lateral point of anterior cranial base (L side)
8	R most anterior lateral part of sphenoid	Most anterior lateral point of sphenoid bone (R side) - where sphenoid, parietal, and frontal bones meet

Landmark #	Name of Landmark	Description
9	L most anterior lateral part of sphenoid	Most anterior lateral point of sphenoid bone (L side) - where sphenoid, parietal, and frontal bones meet
10	R anterior petrous part of temporal bone	Most anterior lateral point of petrous part of temporal bone (R side)
11	L anterior petrous part of temporal bone	Most anterior lateral point of petrous part of temporal bone (L side)
12	R posterior petrous part of temporal bone	Most posterior lateral point of petrous part of temporal bone (R side)
13	L posterior petrous part of temporal bone	Most posterior lateral point of petrous part of temporal bone (L side)
14	R lateral occipital bone	Most lateral point of occipital bone (R side)
15	L lateral occipital bone	Most lateral point of occipital bone (L side)
16	Opisthion	Midpoint of posterior margin of foramen magnum
17	Basion	Midpoint of anterior margin of foramen magnum
18	R midline point of foramen magnum	R most lateral point of foramen magnum

Landmark #	Name of Landmark	Description
19	L midline point of foramen magnum	L most lateral point of foramen magnum
20	R jugular foramen	Most posterior lateral point of margin of R jugular foramen
21	L jugular foramen	Most posterior lateral point of margin of L jugular foramen
22	R internal acoustic meatus	Most posterior lateral point of margin of R internal acoustic meatus
23	L internal acoustic meatus	Most posterior lateral point of margin of L internal acoustic meatus
24	R foramen ovale	Most posterior lateral point of margin of R foramen ovale
25	L foramen ovale	Most posterior lateral point of margin of L foramen ovale
26	R anterior clinoid process	Most superior, posterior and medial point of R anterior clinoid process
27	L anterior clinoid process	Most superior, posterior and medial point of L anterior clinoid process
28	R optic canal	Most posterior lateral point of of margin of R optic canal

Landmark #	Name of Landmark	Description
29	L optic canal	Most posterior lateral point of of margin of L optic canal
30	Foramen Caecum	Most anterior inferior point of anterior midline cranial base
31	Posterior aspect of cribriform plate	Midline point at posterior end of cribriform plate
32	R anterior lateral cribriform	Most anterior and lateral point of cribriform plate (R side)
33	L anterior lateral cribriform	Most anterior and lateral point of cribriform plate (L side)
34	R posterior lateral cribriform	Most posterior and lateral point of cribriform plate (R side)
35	L posterior lateral cribriform	Most posterior and lateral point of cribriform plate (L side)
36	Planum Sphenoidale	Midline point of sphenoidal yoke/planum sphenoidale
37	Tuberculum Sellae	Most convex midline point of tuberculum sellae
38	Dorsum Sellae	Most superior and posterior midline point on dorsum sellae

Landmark #	Name of Landmark	Description
39	Nasion	Most concave point on midline between nasal bone and frontal bone

Table 3: *List of facial landmarks*

Landmark #	Name of Landmark	Description
1	Soft tissue nasion	Most concave point on midline between nasal bridge and forehead
2	Pronasale	Most protruded point of the soft tissue nose
3	Subnasale	Point where the nose connects to the center of upper lip
4	Upper lip	Most anterior point on the curve of the upper lip
5	Stomion	Point at the midline of labial fissure between gently closed lips
6	Lower lip	Most anterior point on the curve of the lower lip
7	Soft tissue B point	Most concave point on the facial midline, between the lower lip and chin
8	Soft tissue pogonion	Most anterior midpoint of the soft tissue chin
9	Soft tissue menton	Most inferior midpoint of the soft tissue chin
10	R medial canthus	Point where the upper and lower eyelids meet nasally (R side)
11	L medial canthus	Point where the upper and lower eyelids meet nasally (L side)

Landmark #	Name of Landmark	Description
12	R lateral canthus	Point where the upper and lower eyelids meet temporally (R side)
13	L lateral canthus	Point where the upper and lower eyelids meet temporally (L side)
14	R alar crease	Most superior point on the alar-facial groove (R side)
15	L alar crease	Most superior point on the alar-facial groove (L side)
16	R alar curvature point	Most lateral point in the curved base line of each ala (R side)
17	L alar curvature point	Most lateral point in the curved base line of each ala (L side)
18	R alar base point	Most inferior point in the curved base line of each ala (R side)
19	L alar base point	Most inferior point in the curved base line of each ala (L side)
20	R nasal ala	Most lateral point on each alar contour (R side)
21	L nasal ala	Most lateral point on each alar contour (L side)

Landmark #	Name of Landmark	Description
22	R cupid bow point	Most elevated point of the philtrum on the upper vermillion border line (R side)
23	L cupid bow point	Most elevated point of the philtrum on the upper vermillion border line (L side)
24	R cheilion	Point located at each labial commissure (R side)
25	L cheilion	Point located at each labial commissure (L side)
26	R malar eminence	Most anteriorly and laterally projecting point of the soft tissue overlying the zygomatic bone (R side)
27	L malar eminence	Most anteriorly and laterally projecting point of the soft tissue overlying the zygomatic bone (L side)
28	R tragus	Most lateral point on tip of tragus of the ear (R side)
29	L tragus	Most lateral point on tip of tragus of the ear (L side)

References

Boughner JC, Wat S, Diewert VM, Young NM, Browder LW, Hallgrímsson B. Short-faced mice and developmental interactions between the brain and the face. J Anat. 2008;213(6):646-662. doi:10.1111/j.1469-7580.2008.00999.x

Bush, Jeffrey O, and Rulang Jiang. “Palatogenesis: morphogenetic and molecular mechanisms of secondary palate development.” *Development (Cambridge, England)* vol. 139,2 (2012): 231-43. doi:10.1242/dev.067082

Gallagher ER, Siebold B, Collett BR, et al. Associations between laterality of orofacial clefts and medical and academic outcomes. *American Journal of Medical Genetics Part A*. 2018;176(4):1037. doi:10.1002/ajmg.a.38663

Hallgrímsson B, Aponte JD, Katz DC, et al. Automated syndrome diagnosis by three-dimensional facial imaging. Genet Med. 2020;22(10):1682-1693. doi:10.1038/s41436-020-0845-y

Jahanbin A, Eslami N, Hoseini Zarch H, Kobravi S. Comparative evaluation of cranial base and facial morphology of cleft lip and palate patients with normal individuals in cone beam computed tomography. J Craniofac Surg. 2015;26(3):785-788. doi:10.1097/SCS.0000000000001361

Marcucio R, Hallgrimsson B, Young NM. Facial Morphogenesis: Physical and Molecular Interactions Between the Brain and the Face. Curr Top Dev Biol. 2015;115:299-320. doi:10.1016/bs.ctdb.2015.09.001

Moore WJ. LCLB. Growth of the facial skeleton in the hominoidea. New York: Academic; 1974.

Neaux D, Wroe S, Ledogar JA, Heins Ledogar S, Sansalone G. Morphological integration affects the evolution of midline cranial base, lateral basicranium, and face across primates. Am J Phys Anthropol. 2019;170(1):37-47. doi:10.1002/ajpa.23899

Parsons TE, Downey CM, Jirik FR, Hallgrimsson B, Jamniczky HA. Mind the gap: genetic manipulation of basicranial growth within synchondroses modulates calvarial and facial shape in mice through epigenetic interactions. PLoS One. 2015;10(2):e0118355. Published 2015 Feb 18. doi:10.1371/journal.pone.0118355

Parsons TE, Schmidt EJ, Boughner JC, Jamniczky HA, Marcucio RS, Hallgrímsson B. Epigenetic integration of the developing brain and face [published correction appears in Dev Dyn. 2011 Dec;240(12):2697]. Dev Dyn. 2011;240(10):2233-2244. doi:10.1002/dvdy.22729

Romash A, Hallgrimsson B, Oberoi S, Young N. (2017). *The Influence of Basicranial Shape on Facial Asymmetry.* [Unpublished manuscript.]

Rutland JW, Bellaire CP, Yao A, et al. The Expanding Role of Geometric Morphometrics in Craniofacial Surgery. *J Craniofac Surg*. 2021;32(3):1104-1109. doi:10.1097/SCS.0000000000007362

Utsunomiya N, Katsube M, Kumakiri M, Morimoto N, Yamada S. Morphological relationship between the cranial base and facial anomalies in humans: Challenges and future perspectives. Congenit Anom. 2025;65(1):e70015. doi:10.1111/cga.70015

Utsunomiya N, Katsube M, Yamaguchi Y, Kumakiri M, Morimoto N, Yamada S. Sella turcica and facial bones: Morphological integration in the human fetal cranium. Orthod Craniofac Res. 2024;00:1-12. doi:10.1111/ocr.12835

Weinberg SM, Andreasen NC, Nopoulos P. Three-dimensional morphometric analysis of brain shape in nonsyndromic orofacial clefting. J Anat. 2009;214(6):926-936. doi:10.1111/j.1469-7580.2009.01084.x

Young NM, Sherathiya K, Gutierrez L, et al. Facial surface morphology predicts variation in internal skeletal shape. Am J Orthod Dentofacial Orthop. 2016;149(4):501-508. doi:10.1016/j.ajodo.2015.09.028

Publishing Agreement

It is the policy of the University to encourage open access and broad distribution of all theses, dissertations, and manuscripts. The Graduate Division will facilitate the distribution of UCSF theses, dissertations, and manuscripts to the UCSF Library for open access and distribution. UCSF will make such theses, dissertations, and manuscripts accessible to the public and will take reasonable steps to preserve these works in perpetuity.

I hereby grant the non-exclusive, perpetual right to The Regents of the University of California to reproduce, publicly display, distribute, preserve, and publish copies of my thesis, dissertation, or manuscript in any form or media, now existing or later derived, including access online for teaching, research, and public service purposes.

Signed by:
Morrina Ron-Sukkawala
66A86308C26B467...
Author Signature

04/17/2026
Date